Acylguanidines as Bioisosteres of Guanidines: N^G-Acylated Imidazolylpropylguanidines, a New Class of Histamine H_2 Receptor Agonists

Prasanta Ghorai,[†] Anja Kraus,[†] Max Keller,[†] Carsten Götte,[†] Patrick Igel,[†] Erich Schneider,[‡] David Schnell,[‡] Günther Bernhardt,[†] Stefan Dove,[†] Manfred Zabel,[§] Sigurd Elz,[†] Roland Seifert,[‡] and Armin Buschauer[†,*]

Departments of Pharmaceutical/Medicinal Chemistry, Pharmacology and Toxicology, Center for Chemical Analysis, Faculty of Chemistry and Pharmacy, University of Regensburg, Universitätsstrasse 31, D-93053 Regensburg, Germany

Received July 9, 2008

N^1-Aryl(heteroaryl)alkyl-N^2-[3-(1*H*-imidazol-4-yl)propyl]guanidines are potent histamine H_2-receptor (H_2R) agonists, but their applicability is compromised by the lack of oral bioavailability and CNS penetration. To improve pharmacokinetics, we introduced carbonyl instead of methylene adjacent to the guanidine moiety, decreasing the basicity of the novel H_2R agonists by 4−5 orders of magnitude. Some acylguanidines with one phenyl ring were even more potent than their diaryl analogues. As demonstrated by HPLC-MS, the acylguanidines (bioisosteres of the alkylguanidines) were absorbed from the gut of mice and detected in brain. In GTPase assays using recombinant receptors, acylguanidines were more potent at the guinea pig than at the human H_2R. At the hH_1R and hH_3R, the compounds were weak to moderate antagonists or partial agonists. Moreover, potent partial hH_4R agonists were identified. Receptor subtype selectivity depends on the imidazolylpropylguanidine moiety (privileged structure), opening an avenue to distinct pharmacological tools including potent H_4R agonists.

Introduction

Histamine receptors (H_1R, H_2R, H_3R, and H_4R) are cell surface receptors and belong to the class 1 or rhodopsin-like family of G-protein coupled receptors, possessing seven transmembrane domains (TMs[a]), three extracellular loops, and three intracellular loops.[1−3] The histamine H_2 receptor (H_2R)[4] is G_s-coupled and therefore activates adenylyl cyclase.[1] H_2Rs are located on gastric parietal cells and in several other tissues and cells including leukocytes, heart, airways, uterus vascular smooth muscles, and in the brain.[1,5,6] Numerous H_2R agonists as well as antagonists have been identified. H_2R antagonists were introduced into the clinic for the treatment of gastroduodenal ulcer and gastresophageal reflux disease. By contrast, H_2R agonists are not routinely used in therapy but are valuable pharmacological tools. Nevertheless, such compounds are of potential therapeutic value as positive inotropic vasodilators for the treatment of acute heart failure,[7] as differentiation-inducing agents in acute myelogenous leukemia,[8] or as anti-inflammatory agents.[9] Compared to amine-type H_2R agonists such as histamine, dimaprit, and amthamine, guanidine-type compounds are much more potent. Impromidine (Figure 1), which is about 50 times more potent than histamine at the guinea pig right atrium, was investigated for the treatment of patients suffering from severe catecholamine-insensitive congestive heart failure.[10,11] Arpromidine (Figure 1) and related *N*-[3-(1*H*-imidazol-4-yl)-propyl]guanidines were developed as positive inotropic vasodilators ("cardiohistaminergics"[12]) and were superior to impromidine in terms of potency and hemodynamic profile when tested in the guinea pig under physiological conditions and in a pathophysiological model of severe congestive heart failure (vasopressin-induced acute heart failure).[7,13,14] Arpromidine and related guanidine-type agonists represent the most potent H_2R agonists known so far, achieving up to 400 times the potency of histamine on the spontaneously beating guinea pig right atrium. The binding site of histamine in the H_2R was identified by in vitro mutagenesis studies and modeling approaches based on the crystal structure of rhodopsin.[15] The interaction of arpromidine and guanidine-type agonists in general may be interpreted by analogy with the model proposed for histamine.[6] The guanidino group undergoes an ionic interaction with Asp-98 in transmembrane domain 3 (TM3), and the imidazole ring forms hydrogen bonds with Asp-186 and Tyr-182 in TM5. Additionally, residues in TM6 like Phe-254 face the imidazolylpropylguanidine moiety of arpromidine.[6,16,17] This binding

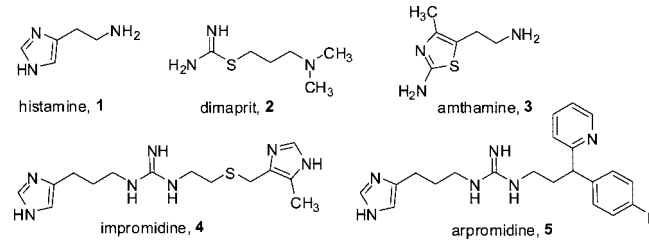

Figure 1. Structures of histamine and selected histamine H_2 receptor agonists.

* To whom correspondence should be addressed. Phone: +49-941 9434827. Fax: +49-941 9434820. E-mail: armin.buschauer@chemie.uni-regensburg.de.

† Pharmaceutical/Medicinal Chemistry, Institute of Pharmacy.

‡ Pharmacology and Toxicology, Institute of Pharmacy.

§ Center for Chemical Analysis, X-ray Laboratory.

[a] Abbreviations: C1, C2, C3, intracellular loops of a GPCR; Cbz, benzyloxycarbonyl; CDI, 1,1′-carbonyldiimidazole; DIPEA, diisopropylethylamine, DMAP, 4-dimethylaminopyridine; DMF, dimethylformamide; DMSO, dimethylsulfoxide; E1, E2, E3, extracellular loops of a GPCR; GTP, guanosine triphosphate; GPCR, G protein-coupled receptor; Gsα, α-subunit of the Gs protein that mediates adenylyl cyclase activation; $G\beta_1\gamma_2$, G protein β_1- and γ_2-subunit; $G\alpha_i$, α-subunit of the Gi protein that mediates inhibition of adenylyl cyclase; gpH_2R, guinea pig histamine H_2 receptor; gpH_2R-GsαS, fusion protein of gpH_2R and Gsα; H_2R, histamine H_2 receptor; H_1R, histamine H_1 receptor; hH_2R, human histamine H_2 receptor; hH_2R-Gsα, fusion protein of the human histamine H_2 receptor and Gsα; hH_3R, human histamine H_3 receptor; hH_4R, human histamine H_4 receptor; hH_4R-RGS19, fusion protein of hH_4R and RGS19; HR-MS, high resolution mass spectrometry; Ms, mesyl, methanesulfonyl; NPY, neuropeptide Y; PE, petroleum ether; RGS, regulator of G protein signaling proteins; SEM, standard error of the mean; SIM, single ion monitoring; TM, transmembrane domain of a GPCR; TFA, trifluoroacetic acid; Tf, triflyl, trifluoromethylsulfonyl; Tr, trityl, triphenylmethyl.

10.1021/jm800841w CCC: $40.75
Published on Web 10/25/2008

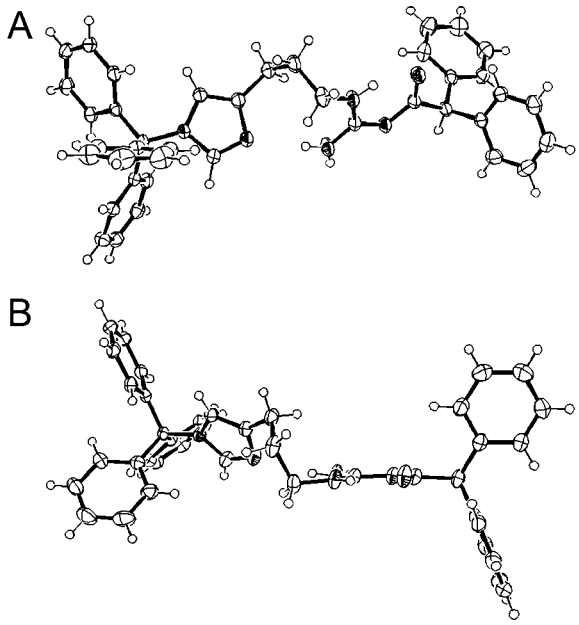

Figure 2. Crystal structure (ORTEP diagram) of trityl-protected acylguanidine **49a** shown in two different views (A and B). CCDC 686506 contains the supplementary crystallographic data for **49a** (available free of charge at The Cambridge Crystallographic Data Centre via www.ccdc.cam.ac.uk/data_request/cif).

site model is generally confirmed using the recent crystal structure of the β_2-adrenoceptor[18,19] as a template (see below). The strongly basic guanidino group, considered a mimic of the primary amino group in histamine, is essential for the H_2R agonistic activity of arpromidine and analogues, but it is also responsible for very low oral bioavailability and lack of penetration across the blood−brain barrier.[13,20,21] This is very unfortunate because, to this end, very little is known about the function of the H_2R in the brain.[22−25] The guanidine-type agonists are nearly quantitatively protonated at physiological pH and are virtually inactive after oral administration. In principle, this problem can be solved by prodrug strategies as demonstrated by the introduction of alkoxycarbonyl groups at the guanidine group.[12] However, such derivatives were not active as H_2R agonists until ester cleavage and decarboxylation. Centrally active H_2R agonists could not be obtained with this approach. The present study describes the successful initial step of developing orally active nonprodrug H_2R agonists as pharmacological tools to investigate the role of the H_2R in the brain. Starting from guanidine-type H_2R agonists, structurally related compounds with reduced basicity were prepared in order to obtain agonists with an improved pharmacokinetic profile. Since structure−activity relationship studies in the arpromidine series revealed that a third substituent on the guanidine group is not tolerated, our attempts focused on modifications of the connecting chains, more precisely, one methylene group adjacent to the guanidine in arpromidine-like H_2R agonists was replaced with an electron-withdrawing carbonyl group. This approach was stimulated by findings in the neuropeptide Y (NPY) receptor field. Specifically, the affinities of N^G-acylated argininamide-type NPY Y_1 antagonists were retained or even increased compared to the respective nonacylated parent compounds.[26−28] The basicity of the acylguanidines (pK_a values around 8) is 4−5 orders of magnitude lower than that of the corresponding guanidines. Hence, on one hand, acylguanidines are sufficiently basic to undergo key interactions with acidic residues of the receptor. On the other hand, a considerable portion remains uncharged at physiological pH, thus facilitating diffusion across membranes. A route for the preparation of N^G-acylated imidazolylpropylguanidines was established, and the synthesized compounds were pharmacologically characterized on isolated guinea pig organs (ileum: H_1R; right atrium: H_2R), on human H_1R-expressing U373-MG cells, and in GTPase assays using membrane preparations of Sf9 insect cells expressing guinea pig (gp) or human (h) histamine receptors. Moreover, absorption after oral administration and brain penetration of representative compounds was explored in nude mice.

Scheme 1. (I) Synthetic Route for the Preparation of the Building Blocks **16**, **17**, and **23**; (II) Synthesis of the Guanidinylation Reagents **13** and **21**[a]

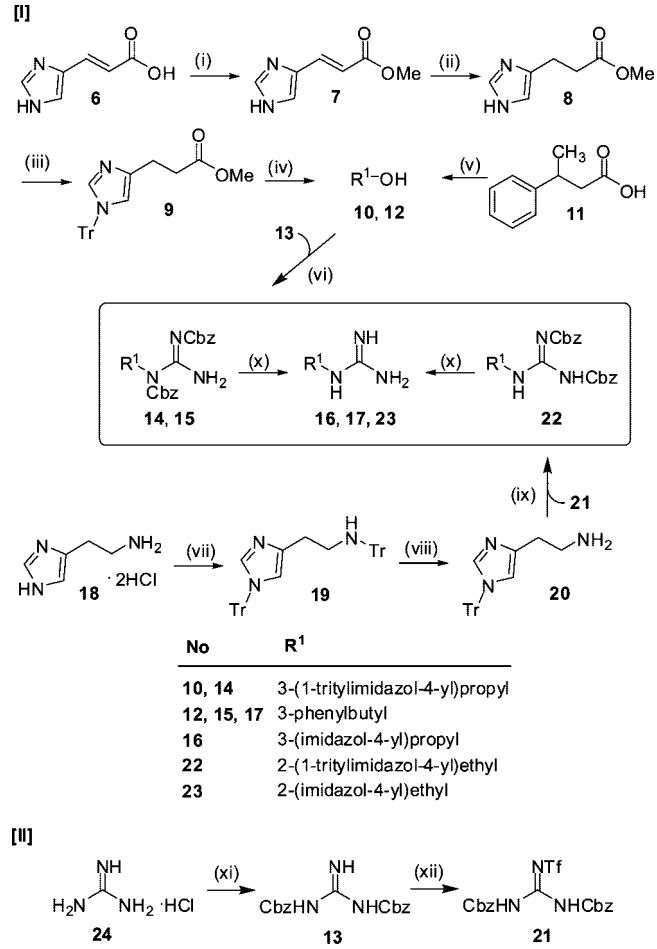

[a] Reagents and conditions: (I) (i) anhydrous Na_2SO_4, H_2SO_4/conc, MeOH/abs, 30 h, reflux; (ii) H_2, Pd/C (10%) (cat.), MeOH, 5 bar, 24 h, rt; (iii) TrCl (1.1 equiv), NEt_3 (2.8 equiv), MeCN, 12 h, rt; (iv) $LiAlH_4$ (2 equiv), THF/abs, Et_2O/abs, 2 h, reflux; (v) $LiAlH_4$ (1.2 equiv), THF/abs, 2 h, rt; (vi) **13** (1.8 equiv), PPh_3 (1.5 equiv), DIAD (1.5 equiv), THF/abs, 24 h, rt; (vii) TrCl, Et_3N, 20 h, 0 °C−rt; (viii) 5% TFA/CH_2Cl_2, 10 min, 0 °C, 45 min, rt; (ix) **21**, Et_3N, CH_2Cl_2, 3 h, rt; (x) H_2, Pd/C (10%), MeOH/THF (1:1), 5 bar, 24 h, rt. (II) (xi) CbzCl, NaOH, CH_2Cl_2/H_2O (2:1), 0 °C, 20 h; (xii) Tf_2O, NaH, THF, −45−0 °C, 16 h.

Chemistry. Toward the synthesis of N^G-acylated guanidines, a guanidine building block is coupled to carboxylic acids to make use of common coupling reagents. The protected alkylated guanidines were prepared starting from alcohols (**10**, **12**) or amine **20** (Scheme 1).[29] Guanidine hydrochloride was treated with sodium hydroxide and benzyloxycarbonyl chloride to yield a nucleophilic guanidinylation reagent (**13**) toward alcohols. The *N*,*N*′-di-Cbz-protected guanidine **13** was subsequently deprotonated with sodium hydride, followed by the treatment with triflic anhydride to provide an electrophilic guanidinylation reagent (**21**) toward amines.

Scheme 2. General Procedures for the Synthesis of Pertinent Carboxylic Acids[a]

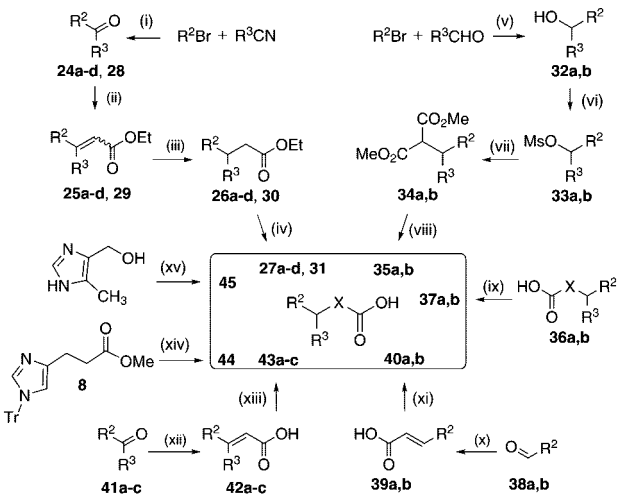

No	R^2	R^3	X	No	R^2	R^3	X
24-27a	Ph	2-pyridyl	CH_2	**37a**	CH_3	cyclohexyl	-
24-27b	4-F-C_6H_4	2-pyridyl	CH_2	**37b**	CH_3	cyclohexyl	CH_2
24-27c	Ph	2-thiazolyl	CH_2	**38-40a**	4-Cl-C_6H_4	4-Cl-C_6H_4	CH_2
24-27d	3,4-diF-C_6H_3	2-thiazolyl	CH_2	**38-40b**	4-Br-C_6H_4	4-Br-C_6H_4	CH_2
28-31	CH_3	2-thienyl	CH_2	**41-43a**	4-F-C_6H_4	4-F-C_6H_4	CH_2
32-35a	CH_3	2-pyridyl	CH_2	**41-43b**	Ph	4-F-C_6H_4	CH_2
32-35b	CH_3	2-thiazolyl	CH_2	**41-43c**	Ph	3,4-diF-C_6H_3	CH_2
36a	CH_3	Ph	-	**44**	H	1-trityl-4-imidazolyl	CH_2
36b	CH_3	Ph	CH_2	**45**	H	5-CH_3-4-imidazolyl	SCH_2

[a] Reagents and conditions: (i) *n*-BuLi, Et_2O, −78 °C, 1 h, rt, overnight; HCl, 0 °C, 20 min; (ii) triethyl phosphonoacetate, NaH, THF, reflux, 24 h; (iii) H_2, Pd/C (10%), MeOH, rt, 24 h; (iv) LiOH, DME/H_2O, rt, 3-5 h; (v) Mg, THF, rt; (vi) MsCl, DMAP, CH_2Cl_2; (vii) DMM, NaH, THF, rt, 12 h; (viii) (a) NaOH, reflux; (b) HCl, reflux, 12 h; (ix) H_2, Rh/Al_2O_3, AcOH, rt, 5−6 bar, 40 h; (x) Ac_2O, NaOAc, reflux, 6 h; (xi) PhCl or PhBr, $AlCl_3$, rt, 3 h; (xii) (a) triethyl phosphonoacetate, KO^{t}Bu, ^{t}BuOH, reflux, 12-16 h; (b) 1 N NaOH, MeOH, reflux, 24h; (xiii) H_2, Pd/C (10%), MeOH, rt, 24 h; (xiv) LiOH/aq (1 N) (1.2 equiv), THF, rt, 24 h; (xv) $HSCH_2COOH$, Na_2CO_3, AcOH, reflux, 24 h.

N-[3-(1-Trityl-1*H*-imidazol-4-yl)propyl]guanidine (**16**) was synthesized starting from urocanic acid (**6**). After esterification, hydrogenation of the double bond and trityl protection of the imidazole NH the ester function was reduced with $LiAlH_4$.[30] The alcohol **10** was coupled to the di-Cbz-protected guanidine **13** under Mitsunobu conditions[29,31] and subsequent cleavage of the protecting groups generated the imidazolylpropylguanidine building block **16**. Starting from 3-phenylbutanoic acid (**11**), the arylalkylguanidine building block **17** was obtained by the reduction of the acid with $LiAlH_4$, yielding **12** followed by subsequent coupling to guanidine **13** and removal of the Cbz-groups by analogy with the aforementioned procedure for compound **16**. The imidazolylethylguanidine building block **23** was synthesized starting from histamine dihydrochloride (**18**). After trityl protection of both imidazole NH and primary NH_2, the side chain of **19** was selectively detritylated by using a low concentration of TFA and the guanidine group was introduced by Goodman's procedure[29] using *N*,*N*′-di-Cbz-*N*″-triflate protected guanidine (**21**) to provide **22**. Again, hydrogenation over Pd/C yielded the imidazolylethylguanidine building block (**23**).

The pertinent alkanoic acids were synthesized by applying standard synthetic methods as summarized in Scheme 2. The ketones **24a**−**d** were prepared from nitriles via the addition of aryl lithium intermediates, which were generated by lithium-halogen exchange from the corresponding heteroaryl bromides, followed by acid hydrolysis. The ketones **24a**−**d** and **28** were treated with triethyl phosphonoacetate to give the compounds **25a**−**d** and **29**, which were subsequently hydrogenated and hydrolyzed to give the 3,3-disubstituted propanoic acids **27a**−**d** and **31**. 1-(Pyridin-2-yl)ethanol (**32a**) was prepared from methylmagnesium bromide and pyridine-2-carbaldehyde. 1-(Thiazol-2-yl)ethanol (**32b**) was synthesized from bromothiazole and acetaldehyde by using known procedures. The alcohols **32a**,**b** were then converted to the mesylates **33a**,**b**, followed by nucleophilic displacement with dimethyl malonate, hydrolysis under alkaline conditions, and decarboxylation to generate the 3-substituted propanoic acids **35a**,**b**. Hydrogenation of the phenylalkanoic acids **36a**,**b** over Rh/Al_2O_3 catalyst resulted in the corresponding cyclohexylalkanoic acids **37a**,**b**. The 4-halobenzaldehydes **38a**,**b** were converted to the 3-(4-halophenyl)-propenoic acids **39a**,**b** and then treated with $AlCl_3$ and aryl halide to provide the acids **40a**,**b**. The 3,3-diarylpropanoic acids **43a**−**c** were prepared via Horner−Wadsworth−Emmons reaction of the corresponding ketones with triethyl phosphonoacetate, followed by in situ hydrolysis and final hydrogenation over Pd/C catalyst. 3-(1-Trityl-1*H*-imidazol-4-yl)propanoic acid (**44**) was prepared by hydrolysis of the corresponding methyl ester **8**. Acid **45** was synthesized from (5-methyl-1*H*-imidazol-4-yl)methanol and sulfanylacetic acid.

According to Scheme 3, the trityl-protected guanidine building blocks (**16**, **17**, **23**) were deprotonated with NaH and coupled to the pertinent carboxylic acids, which were activated with *N*,*N*′-carbonyldiimidazole (CDI) at room temperature. The resulting trityl-protected acylguanidines (**46**−**52a**, **55**−**59a,** **61**−**77a**) were deprotected using trifluoroacetic acid (TFA) to yield the acylguanidines as TFA salts (**46**−**52**, **55**−**59**, **61**−**77**).

The diphenylpropanoylguanidines **53** and **54** (structures see Table 1) were synthesized as previously described.[32] The carboxylic acids **44** and **45** were converted to the acyl chorides, allowed to react with *S*-methylisothiourea to give the corresponding 1-(3,3-diarylpropionyl)-2-methylisothioureas, which were treated with 3-(1*H*-imidazole-4-yl)propylamine to provide N^G-acylated guanidines **53** and **54**. Compound **60** (Table 1) was prepared by hydrogenolytic debenzylation (H_2, Pd/C (10%)) of **59**.

A small sample of intermediate **49a** was isolated and crystallized for X-ray analysis. The crystal structure (view A) shows that a hydrogen bond is possible between the oxygen of amide CO and the hydrogen of that guanidine nitrogen, which is attached to the alkyl group. In view B, the coplanar orientation of the guanidine and the CO group is obvious.

Pharmacological Results and Discussion. The synthesized compounds were investigated for H_2R agonistic activity on the isolated spontaneously beating guinea pig right atrium[4] (positive chronotropic response). Most of the acylguanidines were also investigated for H_1R antagonism on the isolated guinea pig ileum and on U-373 MG human cells. The pharmacological data are summarized in Table 2. A selection of compounds was investigated for H_2R selectivity versus H_1R, H_3R, and H_4R using human and guinea pig histamine receptor models (Table 3) (results of investigations in GTPase assays on hH_2R, gpH_2R, hH_1R, and gpH_1R were already published in part elsewhere[33−38]).

Most of the synthesized acylguanidines were full or nearly full H_2R agonists on the spontaneously beating guinea pig right atrium (Table 2). The suitability of a carbonyl group as a bioisosteric replacement for a methylene group is strongly dependent on the substitution pattern of the H_2R agonist molecule, i.e., the substituents R^2, R^3, and the length of the connecting chain X (see structures in Table 1). As arpromidine and related phenyl(heteroaryl)alkyl substituted imidazolylpropylguanidines are the most potent H_2R agonists known so far,

Scheme 3. General Procedure for Coupling of Acids with Guanidine Building Blocks[a]

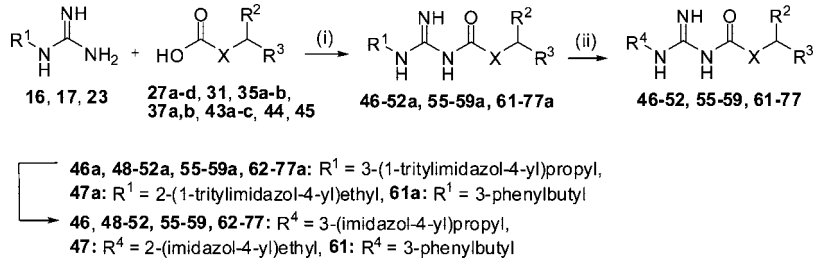

[a] Reagents and conditions: (i) CDI (1.2 equiv), NaH (60% dispersion in mineral oil) (2 equiv), THF/abs, 5 h, rt; (ii) 20% TFA, CH_2Cl_2, 6−10 h, rt. Substitution patterns, see Table 1.

Table 1. Substitution Patterns of Synthesized Acylguanidines **46**−**77**

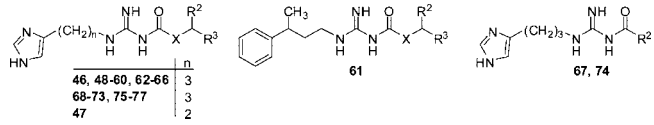

no.	R^2	R^3	X	no.	R^2	R^3	X
46	5-Me-4-imidazolyl	H	CH_2S	**62**	CH_3	Ph	
47	Ph	Ph	CH_2	**63**	CH_3	Ph	CH_2
48	Ph	Ph	CH_2	**64**	CH_3	2-thienyl	CH_2
49	Ph	Ph		**65**	CH_3	2-pyridyl	CH_2
50	4-F-C_6H_4	4-F-C_6H_4	CH_2	**66**	CH_3	2-thiazolyl	CH_2
51	Ph	4-F-C_6H_4	CH_2	**67**	Ph		
52	Ph	3,4-diF-C_6H_3	CH_2	**68**	H	Ph	
53	4-Cl-C_6H_4	4-Cl-C_6H_4	CH_2	**69**	H	Ph	CH_2
54	4-Br-C_6H_4	4-Br-C_6H_4	CH_2	**70**	H	Ph	$(CH_2)_2$
55	2-pyridyl	Ph	CH_2	**71**	H	Ph	$(CH_2)_3$
56	2-pyridyl	4-F-C_6H_4	CH_2	**72**	CH_3	c-hexyl	
57	2-thiazolyl	Ph	CH_2	**73**	CH_3	c-hexyl	CH_2
58	2-thiazolyl	3,4-diF-C_6H_3	CH_2	**74**	c-hexyl		
59	1-benzyl-2-imidazolyl	3,4-diF-C_6H_3	CH_2	**75**	H	c-hexyl	
60	2-imidazolyl	3,4-diF-C_6H_3	CH_2	**76**	H	c-hexyl	CH_2
61	4-imidazolyl	H	CH_2	**77**	H	c-hexyl	$(CH_2)_2$

highest potency was expected to reside in the corresponding acylated analogues, too. "Oxo-arpromidine" (**56**) was 3.5 times less potent than arpromidine (**5**) or half as potent as impromidine (**4**); the intrinsic activity remained unaffected. The oxo-derivative of impromidine (**46**) was likewise nearly as potent as the parent compound (**4**), still acting as a full agonist. The exchange of the *p*-fluoro substituted phenyl ring in "oxo-arpromidine" (**56**) with an unsubstituted phenyl residue (**55**) and further exchange of the 2-pyridyl ring, giving the 3,3-diphenylpropanoyl analogue **48**, resulted in about the same agonistic potency. The introduction of a thiazole ring (**57**) was tolerated as well. In the 3,3-diphenylpropanoyl series, *p*-fluorination and *m*,*p*-difluorination of one ring had a negligible effect on potency (**51** and **52** vs **48**). However, the 3,3-bis(4-fluorophenyl)-derivative (**50**) was about 7 times less potent than the nonhalogenated parent compound **48**. This is different from the structure−activity relationships in nonacylated diphenylpropyl-substituted imidazolylpropylguanidines, where highest potency was found in fluorinated compounds.[20] Fluoro- and chloro- *p*,*p*′-disubstituted diphenylpropanoylguanidines have similar potencies (**50** vs **53**) and are superior to the bromo analogue (**54**). The introduction of different heterocycles instead of an unsubstituted phenyl ring in compound **52** resulted in a similar (**58**, **60**) or lower (**59**) agonistic potency on the guinea pig atrium. In general, unsubstituted or benzyl-substituted imidazole moieties in the side chain of the acylguanidines were less tolerated than a thiazole ring. As in the impromidine or arpromidine series, the trimethylene spacer between imidazole ring and guanidine group represents the optimum. Compound **47**, the shorter homologue of **48**, was significantly less potent and efficacious. Replacement of methylene by carbonyl in this part of the molecule was not tolerated; compound **61**, the constitutional isomer of the 3-phenylbutanoyl analogue **63**, was inactive as an agonist on the guinea pig right atrium.

The tendency toward lower pEC_{50} values of the acylguanidines compared to the alkylguanidines[13,20] was confirmed by investigation of related compounds such as **55**, **57**, **58**, and **60** and was most obvious for the mono- or difluorinated derivatives **50**−**52** and **56**. Nevertheless, it is conceivable that under in vivo conditions reduced potency is compensated by improved pharmacokinetic properties so that a decrease in potency can be accepted to a certain degree. However, a loss of potency is not inevitable. Compounds **48**, **53** and in particular the 3-(hetero)arylbutanoyl substituted guanidines **63**−**66** were as potent as the corresponding 3-(hetero)arylbutylguanidines. The potencies are similar, comparing the alkyl- and the acylguanidine series when one of the aryl rings is replaced with a methyl group. As in the arpromidine series, a three-membered carbon chain between guanidine and aromatic ring is optimal. In the series of N^G-acylated guanidines, the 3-phenylbutanoyl derivative (**63**) was the most potent compound being 64 times more potent than histamine on the guinea pig right atrium. The thienyl (**64**), pyridyl (**65**), and thiazolyl (**66**) analogues are about 26 times more potent than the reference compound still acting as full agonists. In contrast to the alkylguanidine series where the cyclohexyl analogues were about equipotent with the corre-

Table 2. Histamine H_2 Receptor Agonism on the Guinea Pig Right Atrium, H_1 Receptor Antagonism on the Isolated Guinea Pig Ileum, and on U-373 MG Human Cells (Ca^{2+}-Assay)

	histamine H_2 receptor agonism				histamine H_1 receptor antagonism		
	isolated guinea pig right atrium				guinea pig ileum		U-373 MG cells (Ca^{2+}-assay)
no.	pEC_{50}[a] ± SEM	relative potency[b]	E_{max} (%)[c]	N[d]	pA_2 ± SEM (or pD'_2 ± SEM)[e]	N[d]	K_B (μM)[f]
1	6.00 ± 0.02	100	100	>50			
4	7.70 ± 0.10	5000	100	4	5.47 ± 0.01		
5	8.01 ± 0.10	10200	100	5	7.65 ± 0.01	7	
46	7.51 ± 0.09	3200	101 ± 2	4	5.37 ± 0.05	12	8.5
47	6.19 ± 0.17	154	64 ± 3	3	5.01 ± 0.10 [4.55 ± 0.06]	11 16	8.7
48	7.55 ± 0.09	3530	85 ± 3	5	6.13 ± 0.05 [5.20 ± 0.09]	10 18	
49	5.98 ± 0.18	95	69 ± 5	3			4.0
50	6.69 ± 0.07	490	76 ± 2	4	[5.95 ± 0.15]	4	1.4
51	7.26 ± 0.09	1830	95 ± 3	4	[5.39 ± 0.03]	4	
52	7.27 ± 0.05	1850	81 ± 3	4	[6.06 ± 0.14]	4	1.2
53	6.51 ± 0.10	320	60 ± 4	3			
54	6.11 ± 0.10	130	60 ± 4	3			
55	7.29 ± 0.03	1960	97 ± 1	4	4.95 ± 0.04	10	4.9
56	7.47 ± 0.12	2930	100 ± 1	3	5.43 ± 0.03	12	5.2
57	7.42 ± 0.03	2630	100 ± 1	3	5.33 ± 0.05	18	6.8
58	7.30 ± 0.06	2000	90 ± 4	3	5.33 ± 0.07	16	4.6
59	6.40 ± 0.08	251	54 ± 5	3			2.9
60	7.01 ± 0.16	1030	100 ± 4	3			6.2
61	5.19 ± 0.19[g]		7 ± 1[h]	3			9.3
62	5.44 ± 0.20	28	88 ± 5	3	<5.0	2	8.8
63	7.80 ± 0.07	6350	99 ± 2	4	5.87 ± 0.14	4	3.0
64	7.42 ± 0.10	2630	99 ± 2	3			2.1
65	7.42 ± 0.06	2610	98 ± 2	3			7.4
66	7.41 ± 0.11	2590	91 ± 2	4			11.1
67	5.93 ± 0.12	86	89 ± 4	3	>5.0	2	15.8
68	6.74 ± 0.01	546	97 ± 2	3	6.24 ± 0.02	2	2.8
69	6.78 ± 0.10	607	97 ± 5	3	5.67 ± 0.14	5	9.2
70	7.25 ± 0.10	1780	94 ± 2	4	5.74 ± 0.20	2	7.1
71	6.33 ± 0.03	211	86 ± 5	4	6.25 ± 0.03	4	
72	6.86 ± 0.11	729	86 ± 3	3	5.63 ± 0.01	4	8.8
73	7.17 ± 0.07	1470	101 ± 3	3	5.66 ± 0.09	5	0.14
74	7.32 ± 0.07	2090	102 ± 1	3	5.29 ± 0.07	2	6.0
75	7.00 ± 0.10	1000	95 ± 1	3	5.61 ± 0.07	4	4.3
76	7.21 ± 0.11	1610	98 ± 3	3	5.21 ± 0.26	2	1.6
77	6.43 ± 0.06	269	89 ± 7	3	6.13 ± 0.02	4	1.1

[a] pEC_{50} was calculated from the mean shift ΔpEC_{50} of the agonist curve relative to the histamine reference curve by equation: $pEC_{50} = 6.00 + 0.13 + \Delta pEC_{50}$. Summand 0.13 represents the mean desensitization observed for control organs when two successive curves for histamine were performed (0.13 ± 0.02, $N = 16$). The SEM given for pEC_{50} is the SEM calculated for ΔpEC_{50}. [b] Relative potency to histamine = 100%. [c] Efficacy, maximal response (%), relative to the maximal increase in heart rate induced by the reference compound histamine. [d] Number of experiments. [e] pD'_2 values given in brackets for compounds producing a significant, concentration-dependent reduction of histamine's maximal response. [f] K_B values for the inhibition of the histamine (30 μM) induced increase in cellular calcium, mean of two experiments, SEM < 10%. [g] pA_2 (antagonist). [h] E_{max} at 58 μM **61**, E_{max} of histamine in the presence of 58 μM **61** was 45 ± 5%.

Table 3. Agonist/Antagonist Activities on Recombinant Histamine Receptors in GTPase Assays[a]

	hH_1R + RGS4			hH_2R-Gsα[b]			gpH_2R-Gsα[b]		
no.	efficacy	EC_{50}[nM] (K_B[nM])	relative potency	efficacy	EC_{50}(nM) (K_B(nM))	relative potency	efficacy	EC_{50}(nM)	relative potency
1	1.00	190 ± 8.6	100	1.00	1200 ± 300	100	1.00	1,200 ± 200	100
48	0.19 ± 0.02	(2980 ± 719)	6.4	0.69 ± 0.09	78 ± 42	1500	0.93 ± 0.32	6 ± 1	19000
57		(19000 ± 898)	1.0	0.80 ± 0.04	120 ± 45	1000	0.94 ± 0.05	14 ± 4	8570
63	0.35 ± 0.05	(14300 ± 5303)	1.3	0.87 ± 0.01	67 ± 2	1800	1.03 ± 0.06	12 ± 1	10000
64		(10700 ± 1479)	1.8	0.97 ± 0.01	109 ± 31	1156	1.05 ± 0.13	21 ± 19	5710

	hH_3R + Gα_{i2}+ G$\beta_1\gamma_2$ + RGS4			hH_4R-RGS19 + Gα_{i2}+ G$\beta_1\gamma_2$		
no.	efficacy	EC_{50}(nM) (K_B(nM))	relative potency	efficacy	EC_{50}(nM)	relative potency
1	1.00	25.1 ± 3.1	100	1.00	11.6 ± 2.5	100
48		(17.1 ± 1.5)		0.76 ± 0.03	8.6 ± 0.9	135
57		(112.7 ± 4.5)		0.47 ± 0.03	66.3 ± 10.1	17
63	0.24 ± 0.02	2.45 ± 0.65	1024	0.84 ± 0.06	15.3 ± 0.3	76
64	0.29 ± 0.01	1.64 ± 0.96	1530	0.76 ± 0.03	6.3 ± 1.2	184

[a] Membrane preparations of Sf9 insect cells expressing hH_1R (coexpressed with RGS4), hH_2R-$G_{s\alpha}$, or gpH_2R-$G_{s\alpha}$ fusion protein, hH_3R (coexpressed with Gα_i, G$\beta_1\gamma_2$ and RGS4) or hH_4R-RGS19 fusion protein coexpressed with Gα_{i2} G$\beta_1\gamma_2$ were used. Regulator of G-protein signaling proteins (RGS-proteins) enhance agonist-steady-state GTP hydrolysis and, thereby, enhance the signal-to noise ratio of the assays.[59] For experimental protocols, cf. Supporting Information. [b] Data from refs 37, 38 for comparison.

sponding phenyl derivatives,[20] the acylguanidines exhibited different agonistic potencies after introduction of a cyclohexyl ring. Compounds **63** and **73** showed the most pronounced differences: while **63** was 64 times more potent than histamine, the corresponding cyclohexyl analogue **73** was only 15 times more potent than the reference compound.

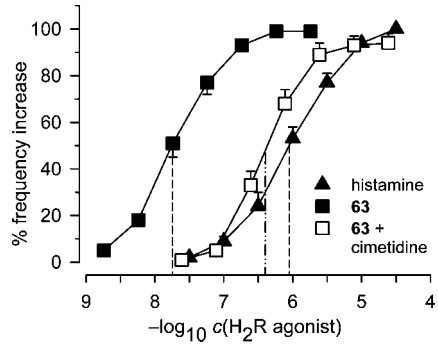

Figure 3. Concentration−response curves on the guinea pig right atrium. Histamine ($pEC_{50} = 6.06 \pm 0.09$, $N = 4$), compound **63** alone ($pEC_{50} = 7.73 \pm 0.07$, relative potency 63.5 (37.7−107.0), $E_{max} = 99 \pm 2\%$, $N = 4$), and **63** in the presence of the H_2R antagonist cimetidine (10 μM, preincubation for 30 min, $pA_2 = 6.31 \pm 0.06$, $N = 3$). Data ± SEM.

Representative concentration−response curves for histamine and compound **63** are shown in Figure 3. The acylguanidine **63** is 64 times more potent than the reference agonist, and the positive chronotropic response is inhibited by the H_2R antagonist cimetidine, resulting in a rightward shift of the concentration−response curve. The pA_2 determined for cimetidine (6.31) versus **63** as the agonist was not significantly different from the values obtained versus other agonists like histamine, impromidine, or arpromidine.

H_2R Binding Model and Species Selectivity. The recently described crystal structures of the β_2-adrenoceptor[18] are suited as a template for homology models of H_2Rs because of the obvious evolutionary relatedness of both receptor subtypes (sequence identity of about 37%). Figure 4 presents a model of the gpH_2R with a focus on the binding site of imidazolylpropylguanidines. Compound **56**, the N^1-acylated analogue of arpromidine, is docked in a favorable extended conformation. Compared to the crystal structure of **49a** (see Figure 2), the spatial arrangement of the N^1-acyl and the N^2-imidazolylpropyl moieties with respect to the guanidino group is changed from $z(N^1)$, $e(N^2)$ into $e(N^1)$, $z(N^2)$. Consequently, the intramolecular H bond of the CO oxygen is formed with the NH_2 moiety of the protonated species. Attempts to dock compound **56** in the arrangement of **49a** were not successful. The docking mode is not essentially different from the mode suggested for arpromidine in a model based on bovine rhodopsin.[17] Compared to carazolol complexed with the β_2-adrenoceptor,[18,19] the position of the heterocycles (imidazole vs. carbazole), and of the basic groups (guanidino carbon vs amino nitrogen) as well as the projection of the side chains (acyl vs isopropyl) principally correspond.

Figure 4A shows that the acylated arpromidine analogue may fit like arpromidine itself into a gpH_2R pocket between TMs 2, 3, 5, 6, and 7. The imidazolylpropyl moiety predominantly contacts amino acids in TMs 5 and 6. The 2-pyridyl group fits to a relatively narrow site mainly formed by TMs 2 and 7. The 4-fluorophenyl moiety may project outward along residues in TM7.

Figure 4B represents the suggested binding mode in more detail. Presumably, the imidazolylpropylguanidine moiety binds to H_2R like histamine (**1**). Studies with H_2R mutants proved an ionic interaction of the protonated amino group of histamine with Asp-98 (3.32).[39] (Numbers in parentheses indicate the generic numbering scheme of amino acids in TMs 1−7 proposed by Ballesteros and Weinstein.[40]) The second and third site of the widely accepted three-point model for biogenic amine/GPCR

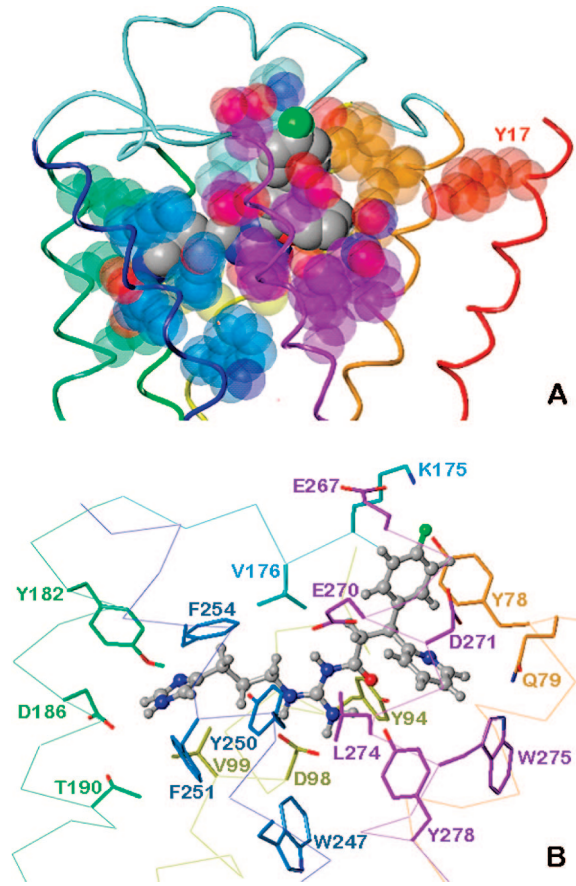

Figure 4. Model of the gpH_2R binding site for compound **56**. Both panels show the side chains and Cα atoms of all amino acids within 3 Å around the ligand and, additionally, the putative toggle switch Trp-247. The backbone and the C atoms of the amino acids are individually drawn in spectral colors: TM1, red; TM2, orange; TM3, yellow; TM4, green; E2, cyan; TM5, greenblue; TM6, blue; TM7, purple. All nitrogens, blue; oxygens, red, C atoms of the ligand, gray. (A) Volume (space fill) representation of the binding site within a tube model of the backbone. Additionally, the gpH_2R specific residue Tyr-17 in TM1 is shown. (B) Detailed model of the gpH_2R-compound **56** interactions. Drawn are the Cα trace (lines), binding site Cα atoms and side chains (sticks), and the ligand (balls and sticks).

interaction could principally be formed by the couples Asp-186/Thr-190 (5.42/5.46)[39] or Tyr-182/Asp-186 (5.38/5.42).[16] Although docking in the first mode is generally possible, too, the pose in Figure 4 reflects the second mode of imidazole binding. This assumption is also in agreement with a pH-dependent model of H_2R activation that suggests subsequent tautomerization of the imidazole ring into the N^{π}-H form caused by neutralization of the imidazole upon binding and accompanied by proton transfers from Tyr-182 to N^{π} and from N^{τ} to Asp-186, respectively.[41] Interactions of nontautomeric agonists with H_2Rs are compatible with this model, too. In conclusion, the suggested binding of the imidazolylpropylguanidine moiety is governed by two H bonds of the imidazole nitrogens with Tyr-182 (5.38) and Asp-186 (5.42), respectively, and by a strong salt bridge or a geometrically favorable charge-assisted H-bond of the guanidino group with the carboxylate function of Asp-98 (3.32). The imidazolylpropyl side chain additionally fits into a pocket consisting of Val-176 (E2), Tyr-250 (6.51), Phe-251 (6.52), and Phe-254 (6.55).

The model predicts that N^1-propanoyl and N^1-propyl chains may fill the same pocket. Because of a possible H bond with the hydroxy group of Tyr-278 (7.43), the CO oxygen should actually lead to higher affinity of the acylated derivatives.

However, in the β_2-adrenoceptor structure, the corresponding tyrosine OH is occupied by a strong intramolecular H bond with the aspartate at position 3.32. On refining the gpH_2R model in complex with compound **56**, Tyr-278 approaches a conformation that rather enables an additional H bond with the guanidine moiety than interaction with the CO oxygen. Another group that may contribute to binding of the acyl oxygen is the hydroxy function of Tyr-94 (3.28).

The suggested pocket for the 2-pyridyl group consists of Gln-79 (2.65), Asp-271 (7.36), Leu-274 (7.39), Trp-275 (7.40), Tyr-278 (7.43) and, possibly through interaction via a water molecule, Tyr-94 (3.28). Trp-275 shapes a boundary of the binding site, disallowing bulky substituents especially in the 4-position. Considering the *p*,*p*′-difluorinated diphenylpropanoylguanidine **50** and its dichlorinated analogue **53**, the potency of the former is much lower when compared with the corresponding bis(4-fluorophenyl)propylguanidine (pEC_{50} of 6.69 vs 7.75[20]), whereas **53** is as potent as its propyl analogue. Thus, the tolerance for a certain bulk is greater in the case of the alkylguanidines compared to the alkanoylguanidines. This finding and, in general, the different structure−activity relationships in both series as well as the mostly lower potency of the acylguanidines must be due to the acyl moiety itself. Because there is no evidence of principally different binding modes and interactions (see above), the most probable reason is the restricted flexibility of the acylguanidines (loss of one freely rotatable bond compared to the alkylguanidine analogues), i.e., the contribution of conformational energy (strain) is simply higher in the case of the present series. This hypothesis is supported by the fact that the 3-phenylbutanoyl analogue **63**, whose methyl group may favorably fit into the "2-pyridyl pocket", has the highest potency within the series.

The *p*-fluorophenyl moiety of compound **56** projects upward into the extracellular region of the gpH_2R and interacts with Tyr-78 (2.64) and Asp-271 (7.36). The slight advantage of the *p*-F substituent (**56** vs **55**) may be due to interactions with Lys-175 (E2) and/or (via water) Glu-267 (7.32).

Although most amino acids interacting with guanidine-type agonists are identical in the human (hH_2R) and guinea pig (gpH_2R) H_2 receptor, the guanidine-type H_2R agonists are less potent and less efficient at the H_2R of human neutrophils than at the H_2R of the guinea pig atrium.[9,13,42] They were also less potent and efficient at hH_2R-$G_{s\alpha S}$ fusion proteins compared to gpH_2R-$G_{s\alpha S}$ fusion proteins in a membrane steady-state GTPase assay, whereas for the small H_2R agonists, such differences were not detected.[17] The model in Figure 4 indicates that Asp-271 in TM7 of the gpH_2R is part of the binding site of the diarylpropanoyl moiety. Asp-271 faces both aryl rings of compound **56** (distance 3 to 4 Å) so that weak anion$-\pi$ interactions are possible just in the case of electron-withdrawing substituents like fluorine. In the hH_2R, this residue is Ala-271, which may in part explain the lower potency at this subtype. Site-directed mutagenesis and previous molecular modeling studies of the gpH_2R suggested that an interaction between Tyr-17 in TM1 and Asp-271 in TM7 accounts for the high efficacy of guanidines. In the light of the β_2-adrenoceptor based model, however, the proposed hydrogen bond[6,17] is unlikely due to the large distance of both residues (see Figure 4A). Possibly this proposed hydrogen bonding can be mediated by water molecules and include Gln-79 (2.65). Such interactions could not occur in the hH_2R possessing Cys-17 and Ala-271 at these positions.[6,17] Hence, the guanidines may stabilize an active conformation in gpH_2R more efficiently and potently than in hH_2R.[17]

The complex of gpH_2R with compound **56** was derived from the inactive state of the β_2-adrenoceptor. A reliable model of the fully active state cannot be obtained without appropriate crystal structures. However, the docking pose in Figure 4 contains interactions probably inducing correlated rotamer changes especially of the aromatic residues Tyr-250 (6.51), Phe-251 (6.52), and Trp-247 (6.48). The tryptophan may serve as toggle switch, leading to subsequent modification of the proline kink in TM6.[18,43] Tyr-250 and Trp-247 are in contact with Leu-274 (7.39) and, via water, the backbone oxygen of Gly-277 (7.42), respectively, suggesting that flexibility of TM7 could also affect the toggle switch. Thus, gpH_2R-selective potency and efficacy may indeed be due to specific interactions of imidazolylpropylguanidines with TM7.

Recently, the N^G-acylated imidazolylpropylguanidines were also investigated in a membrane steady-state GTPase activity assay using fusion proteins of human and guinea pig H_2R and the short splice variant $G_{s\alpha}$, $G_{s\alpha S}$ (selected data in Table 3, for additional data cf. refs 37, 38). Similarly to the results on the guinea pig right atrium, acylguanidines with only one phenyl or cyclohexyl residue show similar or even higher agonistic potencies compared to the diaryl analogues at gpH_2R-$G_{s\alpha S}$ as well as hH_2R-$G_{s\alpha S}$.[37,38] Furthermore, as it was shown for *N*-[3-(1*H*-imidazol-4-yl)propyl]guanidines,[17] the acylated analogues generally activate gpH_2R with higher potency and efficacy than hH_2R.[37,38]

Histamine Receptor Subtype Selectivity. All investigated acylguanidines (**46**−**77**, Table 2) were devoid of histamine H_1R agonistic activity on the guinea pig ileum as well as on human U-373 MG cells. In both test systems, where only weak H_1R antagonism was found, for instance, on the guinea pig ileum, the compounds were 1−2.5 orders of magnitude less potent than the moderate H_1R antagonist arpromidine (**5**).

As shown for a set of representative compounds in Table 3, very weak hH_1R antagonistic (**57**, **64**) or partial agonistic activity (**48**, **63**) was found for most of the acylated imidazolylpropylguanidines studied so far[38] in a steady state GTPase assay on hH_1Rs. By contrast, potent partial agonists at the human hH_4R as well as partial agonists and moderate to potent antagonists at the hH_3R were found among the investigated acylguanidines. This is in agreement with reports on H_3R antagonism,[44,45] H_4R affinity,[46] and H_4R (partial) agonism[47] of the parent guanidine-type H_2R agonist, impromidine. Surprisingly, the imidazolylpropylguanidine portion also confered weak to moderate binding affinity to nonpeptidic NPY Y_1 and Y_4 receptor antagonists.[48,49] Because acylated and nonacylated imidazolylpropylguanidines are both capable of interacting with several targets, these structural moieties may be considered privileged structures.

Brain Penetration of Selected Compounds. The pK_a value of acylguanidinium cations is by 4−5 orders of magnitude lower than that of guanidinium ions (guanidinium: $pK_a \approx 12.5$; acetylguanidinium: $pK_a = 7.6$[50]). On one hand, the acylguanidines are still sufficiently basic to form a cation, which is supposed to interact with Asp-98 in transmembrane domain 3 of the H_2R by analogy with the binding mode suggested for arpromidine-like agonists.[6,17] On the other hand, the reduced basicity of acylguanidines results in penetration across the blood−brain barrier, as a considerable portion of the substance remains uncharged under physiological conditions. This has been shown for the representative compounds **58** and **63** in mice.

As shown in Figure 5 as an example at 15 min after intravenous administration, both compounds (**63**, **58**) were detected in the brain at approximately equimolar concentrations compared to plasma (estimation of teminal half-life in plasma

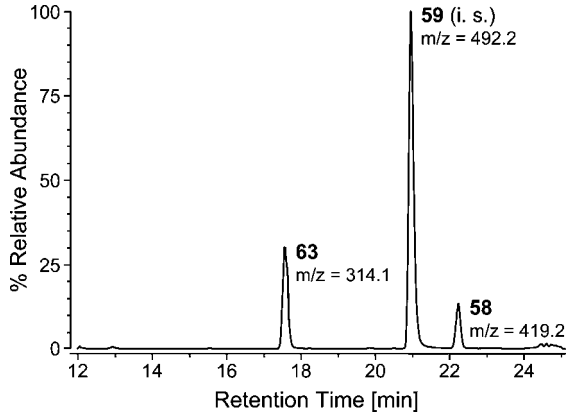

Figure 5. Detection of acylguanidines **58** and **63** by HPLC-MS analysis in the brain of nude mice 15 min after iv administration (i.s. = internal standard; N^1-[3-(1-benzyl-1*H*-imidazol-2-yl)-3-(3,4-difluorophenyl)propanoyl]-N^2-[3-(1*H*-imidazol-4-yl)propyl]guanidine (**59**)). The concentrations in the brain amounted approximately to those in the plasma (data not shown).

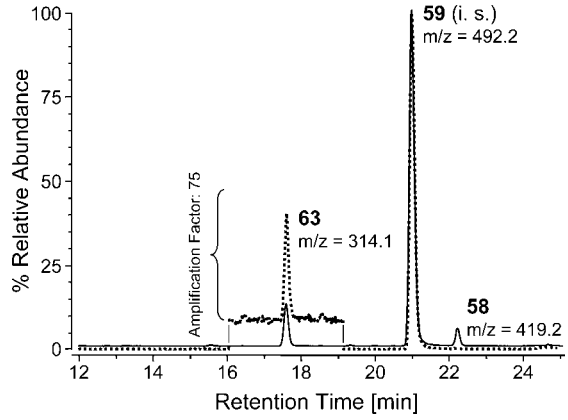

Figure 6. Representative chromatograms of acylguanidines **58** and **63** detected in the plasma of nude mice by HPLC-MS analysis 30 min (dashed line) and 180 min (solid line) after oral administration (i.s. = internal standard; N^1-[3-(1-benzyl-1*H*-imidazol-2-yl)-3-(3,4-difluorophenyl)propanoyl]-N^2-[3-(1*H*-imidazol-4-yl)propyl]guanidine (**59**)).

from preliminary pharmacokinetic experiments: 67 min for **63** and 28 min for **58**).

Resorption of Compounds 58 and 63 after Peroral Administration. Alkylguanidine-type H_2R agonists such as arpromidine had to be converted to prodrugs by introduction of hydrolyzable electron-withdrawing substituents at the third guanidine nitrogen to obtain orally active "cardiohistaminergics".[12] As shown in Figure 6 the conversion of a methylene group adjacent to the guanidine group into a carbonyl group as in **58** and **63** led to absorption from the gastrointestinal tract. Substantial amounts were detected in the plasma of mice after oral administration. As the prototype acylguanidine-type H_2R agonists described in this article are not ideal with respect to receptor selectivity, detailed pharmacokinetic studies will be the subject of future work with optimized compounds.

Conclusion

Alkanoylguanidines and alkylguanidines are bioisosters for H_2Rs, with the acylguanidines exhibiting a basicity 4−5 orders of magnitude lower than that of the parent guanidines. Although a decrease in potency was found when the methylene group in arpromidine-like H_2R agonists was exchanged by a carbonyl group, the new compounds are superior with respect to pharmacokinetic properties. As confirmed by HPLC-MS analysis studies, these compounds are absorbed after oral administration and are capable of penetrating through the blood−brain barrier. Thus, this concept is promising with respect to the development of orally active and centrally available acylguanidines, for instance, as pharmacological tools to study the role of H_2R in the brain. Relatively low receptor subtype selectivity due to the privileged structure, imidazolylpropylguanidine, is characteristic of the compounds presented in this proof-of-concept study. However, the H_2R selectivity of the compounds reported in this study has been overcome by replacing the imidazole ring with other heterocycles (to be reported elsewhere). Moreover, the unexpected high potency of several acylguanidines at HRs other than H_2 provides a sound basis for the further development of ligands with a different receptor profile, for instance, selective tools for the H_4R.

Experimental Section

Where indicated, reactions were carried out under a dry, oxygen-free atmosphere of N_2 using Schlenk technique or under argon atmosphere. Commercially available reagents were used as received. DMF, MeCN, and CH_2Cl_2 were distilled over P_4O_{10} and stored under N_2 over 3 Å molecular sieves. EtOH and MeOH were dried over Mg and stored under N_2. THF, 1,4-dioxane, and Et_2O were dried with Na/benzophenone and stored over Na wire under N_2. EtOAc, PE, $CHCl_3$, CH_2Cl_2, MeOH, and hexane for chromatographic separations were distilled before use. For column chromatography silica gel Geduran 60 (Merck, 0.063−0.200 mm) was used. TLC analysis was done on silica gel 60 F_{254} (Merck) coated on aluminum sheets. NMR spectra were recorded on Bruker Avance 300 (^{1}H: 300 MHz, ^{13}C: 75.5 MHz) and Bruker Avance 600 (^{1}H: 600 MHz; ^{13}C: 150.29 MHz) with TMS as internal standard. X-ray analysis was performed by the Crystallography Laboratory. Elemental analysis (Heraeus Elementar Vario EL III) and mass spectrometry (Finnigan ThermoQuest TSQ 7000) were done by the Central Analytical Laboratory (Universität Regensburg). Preparative chromatography was performed with a Knauer K-1800 pump, using a Eurosphere-100 (250 mm × 32 mm) column, was attached to a Knauer-Detector K-2000 UV detector. The parameters of the preparative chromatography were as follows: UV detection was done at 254 or 210 nm, respectively, temperature was 25 °C, and the flow rate was 40−37 mL/min. The mobile phase was 0.1% TFA in Millipore water and MeOH or MeCN. Analytical chromatography was performed on a system from Thermo Separation Products equipped with a SN 400 controller, P4000 pump, an AS3000 autosampler, and a Spectra Focus UV−vis detector. The columns were either column A: Nucleodur 100−5 C18 (250 mm × 4.0 mm, 5 μm), column B: Luna C18 (150 mm × 4.6 mm, 3 μm), column C: Eurosphere-100 C-18 (250 mm × 4.0 mm, 5 μm) or column D: Purospher 100 C18 (250 mm × 4.0 mm, 5 μm). The temperature was 30 °C, and the UV detection was set to 254 and 210 nm. The mobile phase was 0.05% TFA in Millipore water and MeCN.

Synthetic protocols for the preparation of starting material and analytical data of the following compounds are available as Supporting Information: building blocks **10**, **12**, **13**, **19**−**21, 24a**−**d**, **25a**−**d**, **29**, **26a**−**d**, **30**, **27a**−**d**, **31**, **32a**,**b**, **33a**,**b**, **34a**,**b**, **35a**,**b**, **37a**,**b**, **39a**,**b**, **40a**,**b**, **42a**−**c**, **43a**−**c**, **44**, and **45**, trityl-protected intermediates **47a**−**52a**, **55a**−**59a**, **61a**−**77a**, and acylguanidines **47**−**52**, **55**, **57**−**62**, **65**−**77**.

General Procedure for the Synthesis of *N*,*N*′-Bis(benzyloxycarbonyl)alkylguanidines (14, 15). A solution of the alcohol (11.9 mmol), di-Cbz protected guanidine **13**[29](21.1 mmol), and PPh_3 (18 mmol) in 100 mL of THF/abs was cooled to −5 °C under an argon atmosphere. DIAD (18 mmol) 30 mL THF/abs was added dropwise at such a rate that the reaction mixture was completely colorless before addition of the next drop. After the addition was complete, the reaction mixture was stirred at room temperature for 24 h. The

solvent was removed in vacuo, and the crude product subjected to flash-chromatography.

***N*,*N*′-Bis(benzyloxycarbonyl)-[3-(1-trityl-1*H*-imidazol-4-yl-)propyl]guanidine (14).** Synthesized from **10** and **13**; flash-chromatography (PE/EtOAc 60/40); yield 70%; colorless foam-like solid. ^{1}H NMR ($CDCl_3$) δ (ppm): 7.20−7.48 (m, 20H, Im-2-*H*, Ar-*H*), 7.03−7.14 (m, 6H, Ar-*H*), 6.57 (s, 1H, Im-5-*H*), 5.19 (s, 2H, CH_2Ph), 5.06 (s, 2H, CH_2Ph), 4.02 (t, 2H, J = 7.3 Hz, CH_2N), 2.59 (t, 2H, J = 7.7 Hz, ImCH_2), 1.95 (m, 2H, $CH_2CH_2CH_2$). ES-MS (CH_2Cl_2/MeOH + 10 mM NH_4OAc) *m*/*z* (%): 678 (MH^+, 100); $C_{42}H_{39}N_5O_4$ (677.8).

***N*,*N*′-Bis(benzyloxycarbonyl)-(3-phenylbutyl)guanidine (15).** Synthesized from **12** and **13**; flash-chromatography (PE/EtOAc 90/10); yield 70%; colorless oil. ^{1}H NMR ($CDCl_3$) δ (ppm): 7.36−7.12 (m, 15H, Ar-*H*), 5.16 (s, 2H, CH_2-Ar), 5.15 (s, 2H, CH_2Ar), 3.99−3.77 (m, 2H, CH_2N), 2.74 (m, 1H, CH_3C*H*), 1.89 (m, 2H, CH_3CHCH_2), 1.19 (d, 3H, J = 6.9 Hz, CH_3). ES-MS (CH_2Cl_2/MeOH + 10 mM NH_4OAc) *m*/*z* (%): 460 (MH^+, 100); $C_{27}H_{29}N_3O_4$ (459.5).

***N*,*N*′-Bis(benzyloxycarbonyl)-[2-(1-trityl-1*H*-imidazol-4-yl-)ethyl]guanidine (22).** The amine **20** (1.0 mmol) was added to a solution of **21**[29] (0.9 mmol) and triethylamine (1.0 mmol) in 5 mL of CH_2Cl_2, and the mixture was allowed to stir at room temperature until **21** was consumed (3 h) as evidenced by TLC. After the reaction was complete, the mixture was diluted with CH_2Cl_2 (6 mL) and washed with 2 M sodium bisulfate, saturated sodium bicarbonate, and brine. The organic extract was then dried over sodium sulfate and filtered, and the solvent was removed under reduced pressure. The crude product was further purified by flash column chromatography with CH_2Cl_2. Yield 92%; colorless crystalline solid; mp = 98 °C. ^{1}H NMR ($CDCl_3$) δ (ppm): 11.70 (s, 1H, N*H*), 8.64 (t, J = 5.4 Hz, 1H, N*H*), 7.43 (s, 1H, Im-2-*H*), 7.27−7.40 (m, 19H, Ar-*H*), 7.10−7.16 (m, 6H, Ar-*H*), 6.64 (s, 1H, Im-5-*H*), 5.15 (s, 2H, PhCH_2O), 5.10 (s, 2H, PhCH_2O), 3.74 (dd, J = 6.3 Hz, J = 12.0 Hz, 2H, CH_2NH), 2.81 (t, J = 6.4 Hz, Im-4-CH_2). ES-MS (CH_2Cl_2/MeOH + 10 mM NH_4OAc), *m*/*z*: 664 (MH^+), 243 ($[Ph_3C]^+$); $C_{41}H_{37}N_5O_4$ (663.8).

General Procedure for the Synthesis of the Deprotected Guanidines 16, 17, 23. To a solution of **14**, **15**, or **22** in THF/MeOH (1:1) was added Pd/C (10%), and the mixture was hydrogenated at 5 bar overnight. The mixture was filtered through a small pad of celite, washed with MeOH, and the solvent was removed in vacuo.

***N*-[3-(1-Trityl-1*H*-imidazol-4-yl)propyl]guanidine (16).** Synthesized from **14** (9.7 mmol) using Pd/C (10%) (cat.) in 165 mL THF/MeOH (1:1); yield 98%; pale-yellow foam-like solid. ^{1}H NMR (CD_3OD) δ (ppm): 7.38−7.14 (m, 16H, CPh_3, Im-2-*H*), 6.70 (s, 1H, Im-5-*H*), 3.17 (t, 2H, J = 6.9 Hz, CH_2NH), 2.58 (t, 2H, J = 7.4 Hz, Im-4-CH_2), 1.86 (m, 2H, Im-4-CH_2CH_2). ES-MS (CH_2Cl_2/MeOH + 10 mM NH_4OAc) *m*/*z* (%): 410 (MH^+, 100); $C_{26}H_{27}N_5$ (409.5).

3-Phenylbutylguanidine (17). Synthesized from **15** (2.46 mmol) in 40 mL THF/MeOH (1:1) was added Pd/C (10%) (cat.); yield = 100%; yellow amorphous solid. ^{1}H NMR ($CDCl_3$) δ (ppm): 7.26 (m, 5H, Ar-*H*), 3.03 (t, 2H, J = 7.0 Hz, NHCH_2), 2.81 (m, 1H, CH_3C*H*), 1.88 (m, 2H, CH_3CHCH_2), 1.29 (d, 3H, J = 6.9 Hz, CH_3). CI-MS (NH_3) *m*/*z* (%): 192 (MH^+, 100); $C_{11}H_{17}N_3$ (191.3).

[2-(1-Trityl-1*H*-imidazol-4-yl)ethyl]guanidine (23). Synthesized from **22** (5 mmol) in 15 mL THF: MeOH (1:1) was added Pd/C (10%) (cat.); yield 96%; hygroscopic semisolid. ^{1}H NMR ($CDCl_3$) δ (ppm): 8.51 (s, 1H, N*H*), 7.56 (s, 1H, Im-2-*H*), 7.43−7.01 (m, 15H, Ph-*H*), 6.86 (s, 1H, Im-5-*H*), 3.43 (t, J = 7.1 Hz, 2H, CH_2NH), 3.31 (m, 1H, N*H*), 2.80 (t, J = 7.1 Hz, Im-4-CH_2). ES-MS (CH_2Cl_2/MeOH + 10 mM NH_4OAc), *m*/*z*: 791 ([2 M + H]$^+$), 396 (MH^+), 243 ($[Ph_3C]^+$); $C_{25}H_{25}N_5$ (395.5).

General Procedure for the Preparation of the N^1-acyl-N^2-[1*H*-imidazol-4-yl)alkyl]guanidines (46−52, 55−59, 61−77). Under an argon atmosphere, the pertinent carboxyclic acid (1.0 mmol) was added to a solution of CDI (0.178 g, 1.1 mmol) in DMF or THF (3 mL), and the mixture was stirred at rt for 1 h. At the same time, in a separate flask under argon atmosphere with stirring, sodium hydride (2 mmol, 80 mg of a 60% dispersion in oil) was added to a solution of an imidazolylalkylguanidine (1 mmol) in DMF or THF (5 mL), and the mixture was heated at 50 °C for 30 min and then allowed to cool to rt. The two mixtures were combined and stirred at rt for 5 h, then the solution was poured on water (10 mL) and extracted with EtOAc. The organic phase was washed with saturated sodium bicarbonate and brine, dried over anhydrous Na_2SO_4, and evaporated in vacuo. The residue was purified by a Chromatotron under a NH_3 atmosphere with $CHCl_3$/MeOH as solvent with yields between 70% and 30%. Subsequently, the obtained trityl protected acylguanidines (**46a** not characterized, data of **47a**−**52a**, **55a**−**59a**, **61a**−**77a** cf. Supporting Information) were dissolved in dry CH_2Cl_2 (8 mL), 2 mL of TFA were added drop by drop with constant stirring for 15 min at rt, and stirring was continued till the starting material had completely disappeared (6−10 h). After removing the solvent in vacuo, the residue was purified by preparative HPLC, using mobile phase 0.1% TFA in water and MeOH or MeCN (experimental setup is given at general conditions). All compounds were obtained with yields between 20% and 40% based on the trityl protected products, and their purity was checked by analytical HPLC (experimental setup is given at general conditions, HPLC data available as Supporting Information).

Four representative compounds (**46**, **56**, **63**, **64**) are described in the following, the data of all other acylguanidines prepared according to the general procedure are available as Supporting Information.

***N*^{1}-[2-(5-Methyl-1*H*-imidazol-4-ylmethylsulfanyl)acetyl]-*N*^{2}-[3-(1*H*-imidazol-4-yl)propyl]guanidine (46).** Synthesized from (5-methyl-1*H*-imidazol-4-ylmethylsulfanyl)acetic acid (**45**) and **16** via detritylation of **46a**; yield 54%; sticky oil. ^{1}H NMR (CD_3OD) δ (ppm): 8.81 (s, 1H, Im-2-*H*), 8.75 (s, 1H, Im-2-*H*), 7.37 (s, 1H, Im-5-*H*), 3.95 (s, 2H, SCH_2CO), 3.41−3.33 (m, 2H, NHCH_2), 3.31 (s, 2H, Im-4-CH_2S), 2.90−2.80 (m, 2H, Im-4-CH_2), 2.36 (s, 3H, CH_3), 2.04 (m, 2H, Im-4-CH_2CH_2). ^{13}C NMR (CD_3OD) δ (ppm): 173.4 (quart, *C*O), 155.4 (quart, *C* = NH), 134.9 (+, Im-*C*-2), 134.3 (quart, Im-*C*-4), 134.2 (+, Im-*C*-2), 128.8 (quart, Im-*C*-4), 126.5 (quart, Im-*C*-5), 117.1 (+, Im-*C*-5), 41.6 (−, *C*H_2NH), 35.7 (−, S*C*H_2CO), 27.9 (−, Im-4-CH_2CH_2), 25.0 (−, Im-4-*C*H_2S), 22.5 (−, Im-4-*C*H_2), 8.9 (+, *C*H_3). MS (ESI, CH_2Cl_2/MeOH + 10 mM NH_4OAc): 336 (MH^+). HRMS [FAB(glycerol)]: *m*/*z*, calculated for $[C_{14}H_{21}N_7OS + H]^+$ 336.1601, found, 336.1607; $C_{14}H_{21}N_7OS \cdot 3TFA$ (677.5).

***N*^{1}-[3-(4-Fluorophenyl)-3-(pyridin-2-yl)propanoyl]-*N*^{2}-[3-(1*H*-imidazol-4-yl)-propyl]guanidine (56).** Synthesized from 3-(4-fluorophenyl)-3-(pyridin-2-yl)propanoic acid (**27b**) and **16** via detritylation of **56a**; yield 39%; colorless sticky oil. ^{1}H NMR (CD_3OD) δ (ppm): 8.78 (s, 1H, Im-2-*H*), 8.71 (d, J = 5.2 Hz,1H, Pyr-4-*H*), 8.57 (m, 1H, Pyr-*H*), 8.38 (t, J = 7.8 Hz, 1H, Pyr-*H*), 8.00 (d, J = 8.2 Hz, 1H, Pyr-*H*), 7.78 (t, J = 6.7 Hz, 1H, Ph-*H*), 7.50−7.40 (m, 2H, Ph-*H* and Im-*H*), 7.09 (t, J = 7.8 Hz, 2H, Ph-*H*), 4.84 (t overlap with H_2O, 1H, Ar_2CH), 3.68 (dd, J = 9.0 Hz, J = 17.3 Hz, 1H, CH*H*CO), 3.43 (dd, J = 6.6 Hz, J = 17.3 Hz, 1H, C*H*HCO), 3.35−3.30 (m, 2H, NHCH_2), 2.82 (t, J = 7.5 Hz, 2H, Im-4-CH_2), 2.00 (m, 2H, Im-4-CH_2CH_2). ^{13}C NMR (CD_3OD) δ (ppm): 174.4 (quart, *C*O), 163.7 (quart, d, J = 246.1 Hz, *C*F), 159.8 (quart, Py-*C*-2), 155.1 (quart, *C* = NH), 146.2 (+, Py-*C*-6), 144.5 (+, Im-*C*-2), 136.3 (quart, Ar-*C*-1), 134.9 (+, Pyr-*C*-4), 134.2 (quart, Im-*C*-4), 131.1 (+, d, J = 8.2 Hz, 2C, Ar-*C*-2/-6), 126.6 (+, Pyr-*C*-3), 125.9 (+, Pyr-*C*-5), 117.1 (+, d, J = 21.1 Hz, 2C, Ar-*C*-3/-5), 117.0 (+, Im-*C*-5), 45.9 (+, $COCH_2CH$), 41.8 (−, $COCH_2$), 41.6 (−, $NHCH_2$), 28.0 (−, Im-4-CH_2CH_2), 22.4 (−, Im-4-*C*H_2). ES-MS (CH_2Cl_2/MeOH + 10 mM NH_4OAc): 395 (MH^+). HRMS [EI-MS]: *m*/*z*, calculated for $[C_{21}H_{23}FN_6O]$ 394.1917, found, 394.1917; $C_{21}H_{23}FN_6O \cdot 3TFA$ (736.5).

***N*^{1}-[3-(1*H*-Imidazol-4-yl)propyl]-*N*^{2}-(3-phenylbutanoyl)guanidine (63).** Synthesized from 3-phenylbutanoic acid and **16** via detritylation of **63a**; yield: 20%; colorless sticky oil. ^{1}H NMR (CD_3OD) δ (ppm): 8.77 (d, 1H, J = 1.3 Hz, Im-2-*H*), 7.34 (s, 1H, Im-5-*H*), 7.18−7.27 (m, 5H, Ph), 3.33 (m, 3H, Im-4-$CH_2CH_2CH_2$, $COCH_2CH$), 2.78 (m, 4H, Im-4-CH_2CH_2, $COCH_2$), 2.00 (m, 2H, Im-4-CH_2CH$_2$), 1.31 (d, 3H, J = 7.0 Hz, CH_3). ^{13}C NMR (CD_3OD)

δ (ppm): 176.02 (quart, *C*O), 155.31 (quart, *C*═NH), 146.41 (quart. Ph-*C*-1), 134.93 (+, Im-*C*-2), 134.30 (quart, Im-*C*-4), 127.67, 127.95, 129.63 (+, arom. *C*H), 116.96 (+, Im-*C*-5), 46.06 (−, $COCH_2$), 41.49 (−, Im-4-$CH_2CH_2CH_2$), 37.63 (+, $COCH_2CH$), 27.91 (−, Im-4-CH_2CH_2), 23.49 (−, Im-4-CH_2CH_2), 22.20 (+, CH_3). HRMS: EI-MS: *m*/*z* for $[C_{17}H_{23}N_5O]$ calcd 313.1903, found 313.1902; $C_{17}H_{23}N_5O \cdot 2TFA$ (541.4).

***N*¹-[3-(1*H*-Imidazol-4-yl)propyl]-*N*²-[3-(thiophen-2-yl)butanoyl]guanidine (64).** Synthesized from (3-thiophen-2-yl)butanoic acid (**31**) and **16** via detritylation of **64a**; yield 43%; colorless sticky oil. ^{1}H NMR (CD_3OD) δ (ppm): 8.84 (s, 1H, Im-2-*H*), 7.48 (s, 1H, Im-5-*H*), 7.30 (m, 1H, Thio-*H*), 6.93 (m, 2H, Thio-*H*), 3.60 (m, 1H, $COCH_2CH$), 3.32 (m, 2H, $NHCH_2$), 2.92 (m, 4H, Im-4-CH_2 and one of $COCH_2$), 2.00 (m, 2H, Im-4-CH_2CH_2), 1.42 (d, *J* = 7.0 Hz, 3H, CH_3). ^{13}C NMR (CD_3OD) δ (ppm): 175.6 (quart, *C*O), 155.2 (quart, *C*═NH), 150.0 (+, Thio-*C*-2), 134.9 (+, Im-*C*-2), 134.3 (quart, Im-*C*-4), 127.7 (+, Thio-*C*-5), 126.3, 124.4 (+, Thio-*C*-3,4), 117.1 (+, Im-*C*-5), 47.0 (−, $CHCH_2CO$), 41.6 (−, CH_2NH), 32.9 (+, $CHCH_2CO$), 27.9 (−, Im-4-CH_2CH_2), 23.2 (+, CH_3), 22.5 (−, Im-4-CH_2). MS (ESI, CH_2Cl_2/MeOH + 10 mM NH_4OAc): *m*/*z* 320 (MH^+). HRMS: EI-MS: *m*/*z* for $[C_{15}H_{21}N_5OS]$ calcd 319.1467, found 319.1469; $C_{15}H_{21}N_5OS \cdot 2TFA$ (547.5).

General Procedure for the Preparation of the *N*¹-(3,3-diphenylpropanoyl)-*N*²-[1*H*-imidazol-4-yl)propyl]guanidines 53, 54.[32] The corresponding *p*,*p*′-dihalogenated 1-(3,3-diphenylpropanoyl)-2-methylisothiourea (1 mmol), prepared from the respective carboxylic acid chloride and *S*-methylisothiourea hydroiodide in the presence of triethylamine (2 equiv) in acetone at rt, was dissolved in 10 mL of anhydrous MeCN and added to a solution of 3-(1*H*-imidazol-4-yl)propylamine in 10 mL MeCN. The mixture was stirred for 14 h at 60 °C, the solvent subsequently removed in vacuo, redissolved in very little 0.1 N HCl/aq, and the solvent immediately removed in vacuo. The remaining foam was repeatedly dissolved in EtOH and the solvent removed in vacuo. The residue was purified by a Chromatotron using $CHCl_3$/MeOH (7:1).

***N*¹-[3,3-Bis(4-chlorophenyl)propanoyl]-*N*²-[3-(1*H*-imidazol-4-yl)propyl]guanidine (53).** Synthesized from 1-[3,3-bis(4-chlorophenyl)propanoyl]-2-methylisothiourea and 3-(1*H*-imidazol-4-yl)propylamine; yield 33%; colorless hygroscopic foam. ^{1}H NMR (DMSO-d_6) δ (ppm): 14.40 (br, 2H, NH_2), 12.40 (s, 1H, N*H*), 9.06 (br, 1H, N*H*), 9.00 (s, 1H, Im-2-*H*), 7.45 (s, 1H, Im-5-*H*), 7.26−7.40 (m, 8H, Ar-*H*), 4.60−4.69 (m, 1H, Ar_2CH), 3.11−3.37 (m, 4H, Ar_2CHCH_2, $NHCH_2$), 2.49 (d, *J* = 7.5 Hz, 2H, Im-4-CH_2), 1.81−1.90 (m, 2H, Im-4-CH_2CH_2). HRMS (FAB^+, CH_2Cl_2, MeOH) *m*/*z*, calculated for $[C_{22}H_{23}Cl_2N5O]$ 444.1357, found, 444.1351; $C_{22}H_{23}Cl_2N_5O \cdot 2$ TFA (672.4).

***N*¹-[3,3-Bis(4-bromophenyl)propanoyl]-*N*²-[3-(1*H*-imidazol-4-yl)propyl]guanidine (54).** Synthesized from 1-[3,3-bis(4-bromophenyl)propanoyl]-2-methylisothiourea and 3-(1*H*-imidazol-4-yl)propylamine; yield 48%; colorless hygroscopic foam. ^{1}H NMR (DMSO-d_6) δ (ppm): 14.40 (br, 2H, NH_2), 12.40 (s, 1H, N*H*), 9.10 (br, 1H, N*H*), 9.02 (s, 1H, Im-2-*H*), 7.42−7.56 (m, 4H, Ar-*H*, Im-5-*H*), 7.25−7.35 (m, 4H, Ar-*H*), 4.62 (*app*-t, *J* = 7.9 Hz, 1H, Ar_2CH), 3.20−3.30 (m, 4H, Ar_2CHCH_2, $NHCH_2$), 2.62−2.71 (m, 2H, Im-4-CH_2), 1.80−1.91 (m, 2H, Im-4-CH_2CH_2). HRMS (FAB^+, CH_2Cl_2, MeOH) *m*/*z*, calculated for $[C_{22}H_{23}Br_2N_5O]$ 532.0347, found, 532.0347; $C_{22}H_{23}Br_2N_5O \cdot 2TFA$ (761.3).

Analysis of Compounds 63 and 58 in Brain and Blood. Detection in Brain after Systemic Administration. To investigate the penetration of **63** and **58** across the blood−brain barrier, a mixture of these compounds was administered to male nude mice (nu/nu, weight: 30−35 g) by retrobulbar injection in an isotonic solution of sodium chloride (final DMSO concentration: 10%) at a dosage of 10 mg/kg each (concentration: 2 + 2 mg/mL, injected volume: 50 μL/10 g mouse). Mice were killed 15 min after injection by cardiac puncture during anesthesia with sevofluran, followed by removal of the brains. The tissues were homogenized (1000 rpm, on ice) in 1% aqueous TFA (150 mg tissue/1 mL) with a Potter−Elvehjem homogenizer (type 8, 5 mL-vessel, Teflon pestle, Braun, Melsungen, Germany). One mL of the homogenate was mixed vigorously with the internal standard (**59**), followed by the addition of 100 μL of acetonitrile, mixing, and centrifugation (13000 rpm, 5 min, Biofuge 13, Heraeus, Germany). After removal of the supernatants, residues were resuspended in 1 mL of 1% aqueous TFA and 100 μL of acetonitrile, mixed, and centrifuged. Solid phase extraction cartridges (Strata-X-C, 3 mL, 60 mg, Phenomenex, Aschaffenburg, Germany), conditioned with 2 mL of methanol and 2 mL of water, were loaded with the combined supernatants. Washing was performed with 2 mL of hydrochloric acid (0.1 N) and 2 mL of a mixture of water and methanol (95/5). Cartridges were dried prior to elution with 3 mL of an ammonia enriched (3.5 N) mixture of acetonitrile and methanol (50/50). The eluates were evaporated in a vacuum concentrator (Speed-Vac Plus, Egelsbach, Germany), residues were dissolved in 300 μL of a mixture of acetonitrile and 0.1% TFA in water (20/80), filtered (0.45 μm), and injected into the LC-MS system (LC: Agilent 1100, Palo Alto, CA; MS: TSQ 7000, Thermo FINNIGAN, USA). HPLC conditions: column: Synergi Hydro RP (250 mm × 4.6 mm, 4 μm, Phenomenex, Aschaffenburg, Germany), mobile phase: mixtures of acetonitrile (A) and 0.1% TFA in water (B), gradient: 0−6 min: A/B: 20/80, 6−20 min: A/B: 20/80 → 32/68, 20−20.5 min: A/B: 32/68 → 80/20, 20.5−25 min: A/B: 80/20, flow rate: 0.8 mL/min, oven temperature: 45 °C, UV-detection: 214 nm, injection: 50 μL. MS-conditions: single ion monitoring (SIM), source type: ESI (capillary temperature: 350 °C, spray voltage: 4.0 kV, sheath and auxiliary gas: on).

Absorption after Oral Administration. A mixture of **63** and **58** was administered to male nude mice (nu/nu, weight: 30−35 g) by gavage at a dose of 5 mg/kg each in isotonic sodium chloride solution ((final DMSO concentration: 5%). Blood was collected by cardiac puncture during sevofluran anesthesia and centrifuged. Heparin plasma (200 μL) was used for sample preparation. After addition of the internal standard **(59)**, proteins were precipitated by addition of 400 μL of ice-cold acetonitrile, strong mixing, incubation at −20 °C for 30 min, and additional vigorous mixing. After centrifugation at 5 °C (4000 rpm, 5 min, MinifugeT, Heraeus, Hanau, Germany), supernatants were transferred to 1.5 mL reaction vessels (Eppendorf, Hamburg, Germany) and residues were washed with 300 μL of ice-cold acetonitrile followed by centrifugation. Combined supernatants were evaporated to dryness in a vacuum concentrator (Speed-Vac Plus, Egelsbach, Germany), residues were dissolved in 300 μL of a mixture of acetonitrile and 0.1% TFA in water (20/80), filtered (0.45 μm), and analyzed by LC-MS as described above.

Pharmacological Methods. The experimental protocols for the determination of pharmacological parameters on the guinea pig right atrium (H_2R), the guinea pig ileum (H_1R), U373-MG cells (hH_1R, calcium assay), the GTPase assays on membrane preparations of Sf9 cells expressing the human H_1, H_2, H_3, or H_4 receptor, or the guinea pig H_2R, follow the standard procedures provided as Supporting Information.

Data Handling and Pharmacological Parameters. Data presented as mean ± SEM or SE or with 95% confidence limits (cl) unless otherwise indicated. Agonist potencies are given in percent or are expressed as pEC_{50} values (negative decadic logarithm of the molar concentration of the agonist producing 50% of the maximal response) and were corrected according to the long-term mean value of the reference agonist histamine in our laboratory (guinea pig atrium (H_2): pEC_{50} = 6.00 for histamine). Maximal responses are expressed as E_{max} values (percentage of the maximal response to histamine as reference). Antagonist affinities are expressed apparent pA_2 values and were calculated from the following equation: $pA_2 = -\log c(B) + \log(r - 1)$, where $c(B)$ is the molar concentration of antagonist and *r* the ratio of agonist EC_{50} measured in the presence and absence of antagonist.[51,52] Noncompetitive antagonists are characterized by estimation of a pD'_2 value according to the equation: $pD'_2 = -\log c(B) + \log(100/E_{max} - 1)$.[53] Where appropriate, differences between means were determined by Student's *t* test, after checking the homogeneity of the variances; *P* values <0.05 were considered to indicate a significant difference between the mean values being compared.

K_B values for H_1R antagonism in the calcium assay (U373-MG cells) were calculated from IC_{50} values according to the Cheng−Prusoff equation.[54]

Molecular Modeling. First, a rough model of gpH_2R was directly constructed from the PDB file 2RH1 of the β_2-adrenoceptor crystal structure.[18] The backbone coordinates of TMs 1−7, helix 8, the loops C1, E1, and C2, corresponding parts of E2, intrahelical water molecules, as well as identical side chains were retained. All other cocrystallized substructures and the lysozyme domain were deleted. The beginning (Lys-227−Val-242) and the end (Phe-264−Glu-268) of the C3 loop were replaced by the corresponding parts of the crystal structure 2R4R[55] (the free state of these positions is probably better represented by the complex with a Fab than by a covalent construct). Also the C terminus was added from the 2R4R file. The remainder of the E2 and C3 loops, the E3 loop and the motif between TM7 and TM8 were constructed by Sybyl loop searches. The side chains differing between the β_2-adrenoceptor and the gpH_2R were mutated.

The resulting rough model was prepared for optimization by adding hydrogens and providing atoms with Amber-FF99 charges.[56] Bad contacts of side chains were removed using the Lovell rotamer library.[57] Subsequently, the model was roughly minimized by the steepest descent method (200 cycles, Amber-FF99 force field,[56] distant dependent dielectric constant of 4). In the first 100 steps, the backbone of the TMs was fixed. Compound **56** was manually docked into the model in an extended, energetically favorable conformation, considering results of previous in vitro mutagenesis and theoretical studies.[6,16,17,39,41] The complex was first minimized with the Amber-FF99 force field (ligand fixed and provided with Gasteiger−Hueckel charges, distant dependent dielectric constant of 4, 20 cycles steepest descent, then Powell algorithm) down to an rms gradient of less than 0.05 kcal mol^{-1} $Å^{-1}$. The final minimization considered compound **56** and a region of 6 Å around (combined organic−protein MMFF94 force field[58] and charges, distant dependent dielectric constant of 1, Powell method, rms gradient criterion 0.05 kcal mol^{-1} $Å^{-1}$). The rms deviation of the TM backbones between the resulting model and the β_2-adrenoceptor crystal structure 2RH1 amounts to 0.68 Å. All calculations were performed with SYBYL 7.3 (Tripos, St. Louis, MO) on a SGI Octane workstation.

Acknowledgment. We are grateful to Dr. Hendrik Preuss for helpful discussion and Astrid Seefeld, Gertraud Wilberg, Elvira Schreiber, Christine Braun, and Kerstin Röhrl for expert technical assistance. This work was supported by the Graduate Training Program (Graduiertenkolleg) GRK 760, "Medicinal Chemistry: Molecular Recognition−Ligand−Receptor Interactions", of the Deutsche Forschungsgemeinschaft.

Supporting Information Available: Synthetic protocols and analytical data of the compounds **10**,**12**,**13**, **19**−**21**, **24a**−**d**, **25a**−**d**, **29**, **26a**−**d**, **30**, **27a**−**d**, **31**, **32a**,**b**,**33a**,**b**,**34a**,**b**,**35a**,**b**,**37a**,**b**,**39a**,**b**, **40a**,**b**, **42a**−**c**, **43a**−**c**, **44**,**45**, **47a**−**52a**,**55a**−**59a**, **61a**−**77a**, **47**−**52**, **55**, **57**−**62**, **65**−**77**, HPLC data for the acylguanidines **46**−**77**, tracings of key target compounds, and pharmacological methods. The supplementary crystallographic data for compound **49a** can be obtained free of charge from The Cambridge Crystallographic Data Centre via www.ccdc.cam.ac.uk/data_request/cif, deposition number CCDC 686506. This material is available free of charge via the Internet at http://pubs.acs.org.

References

(1) Hill, S. J.; Ganellin, C. R.; Timmerman, H.; Schwartz, J.-C.; Shankley, N. P.; Young, J. M.; Schunack, W.; Levi, R.; Haas, H. L. International Union of Pharmacology. XIII. Classification of Histamine Receptors. *Pharmacol. Rev.* **1997**, *49*, 253–278.

(2) Hough, L. B. Genomics Meets Histamine Receptors: New Subtypes, New Receptors. *Mol. Pharmacol.* **2001**, *59*, 415–419.

(3) Foord, S. M.; Bonner, T. I.; Neubig, R. R.; Rosser, E. M.; Pin, J.-P.; Davenport, A. P.; Spedding, M.; Harmar, A. J. International Union of Pharmacology. XLVI. G Protein-Coupled Receptor List. *Pharmacol. Rev.* **2005**, *57*, 279–288.

(4) Black, J. W.; Duncan, W. A.; Durant, C. J.; Ganellin, C. R.; Parsons, E. M. Definition and antagonism of histamine H_2-receptors. *Nature (London)* **1972**, *236*, 385–390.

(5) Traiffort, E.; Pollard, H.; Moreau, J.; Ruat, M.; Schwartz, J.-C.; Martinez-Mir, M. I.; Palacios, J. M. Pharmacological Characterization and Autoradiographic Localization of Histamine H_2 Receptors in Human Brain Identified with [^{125}I]Iodoaminopotentidine. *J. Neurochem.* **1992**, *59*, 290–299.

(6) Dove, S.; Elz, S.; Seifert, R.; Buschauer, A. Structure−Activity Relationships of Histamine H_2 Receptor Ligands. *Mini-Rev. Med. Chem.* **2004**, *4*, 941–954.

(7) Felix, S. B.; Buschauer, A.; Baumann, G. Therapeutic value of H_2-receptor stimulation in congestive heart failure. Hemodynamic effects of BU-E-76, BU-E-75 and arpromidine (BU-E-50) in comparison to impromidine. *Agents Actions Suppl.* **1991**, *33*, 257–269.

(8) Seifert, R.; Hoer, A.; Schwaner, I.; Buschauer, A. Histamine increases cytosolic Ca^{2+} in HL-60 promyelocytes predominantly via H_2 receptors with an unique agonist/antagonist profile and induces functional differentiation. *Mol. Pharmacol.* **1992**, *42*, 235–241.

(9) Burde, R.; Buschauer, A.; Seifert, R. Characterization of histamine H_2-receptors in human neutrophils with a series of guanidine analogues of impromidine. *Naunyn-Schmiedeberg's Arch. Pharmacol.* **1990**, *341*, 455–461.

(10) Baumann, G.; Felix, S. B.; Heidecke, C. D.; Rieβ, G.; Loher, U.; Ludwig, L.; Blömer, H. Apparent superiority of H_2-receptor stimulation and simultaneous β-blockade over conventional treatment with β-sympathomimetic drugs in post-acute myocardial infarction: Cardiac effects of impromidine—a new specific H_2-receptor agonist—in the surviving catecholamine-insensitive myocardium. *Inflamm. Res.* **1984**, *15*, 216–228.

(11) Baumann, G.; Permanetter, B.; Wirtzfeld, A. Possible value of H_2-receptor agonists for treatment of catecholamine-insensitive congestive heart failure. *Pharmacol. Ther.* **1984**, *24*, 165–177.

(12) Mörsdorf, P.; Engler, H.; Schickaneder, H.; Buschauer, A.; Schunack, W.; Baumann, G. Cardiohistaminergics—new developments in histamine H_2-agonists. *Drugs Future* **1990**, *15*, 919–933.

(13) Buschauer, A. Synthesis and in vitro pharmacology of arpromidine and related phenyl(pyridylalkyl)guanidines, a potential new class of positive inotropic drugs. *J. Med. Chem.* **1989**, *32*, 1963–1970.

(14) Buschauer, A.; Baumann, G. Structure−activity relationships of histamine H_2-agonists, a new class of positive inotropic drugs. *Agents Actions Suppl.* **1991**, *33*, 231–256.

(15) Palczewski, K.; Kumasaka, T.; Hori, T.; Behnke, C. A.; Motoshima, H.; Fox, B. A.; Trong, I. L.; Teller, D. C.; Okada, T.; Stenkamp, R. E.; Yamamoto, M.; Miyano, M. Crystal Structure of Rhodopsin: A G Protein-Coupled Receptor. *Science* **2000**, *289*, 739–745.

(16) Nederkoorn, P. H. J.; Gelder, E. M.; Donné-Op den Kelder, G. M.; Timmerman, H. The agonistic binding site at the histamine H_2 receptor. II. Theoretical investigations of histamine binding to receptor models of the seven α-helical transmembrane domain. *J. Comput.-Aided Mol. Des.* **1996**, *10*, 479–489.

(17) Kelley, M. T.; Bürckstümmer, T.; Wenzel-Seifert, K.; Dove, S.; Buschauer, A.; Seifert, R. Distinct interaction of human and guinea pig histamine H_2-receptor with guanidine-type agonists. *Mol. Pharmacol.* **2001**, *60*, 1210–1225.

(18) Cherezov, V.; Rosenbaum, D. M.; Hanson, M. A.; Rasmussen, S. G.; Thian, F. S.; Kobilka, T. S.; Choi, H. J.; Kuhn, P.; Weis, W. I.; Kobilka, B. K.; Stevens, R. C. High-resolution crystal structure of an engineered human beta2-adrenergic G protein-coupled receptor. *Science* **2007**, *318*, 1258–1265.

(19) Rosenbaum, D. M.; Cherezov, V.; Hanson, M. A.; Rasmussen, S. G.; Thian, F. S.; Kobilka, T. S.; Choi, H. J.; Yao, X. J.; Weis, W. I.; Stevens, R. C.; Kobilka, B. K. GPCR engineering yields high-resolution structural insights into beta2-adrenergic receptor function. *Science* **2007**, *318*, 1266–1273.

(20) Buschauer, A.; Friese-Kimmel, A.; Baumann, G.; Schunack, W. Synthesis and histamine H_2 agonistic activity of arpromidine analogues: replacement of the pheniramine-like moiety by nonheterocyclic groups. *Eur. J. Med. Chem.* **1992**, *27*, 321–330.

(21) Durant, G. J.; Duncan, W. A. M.; Ganellin, C. R.; Parsons, M. E.; Blakemore, R. C.; Rasmussen, A. C. Impromidine (SKF 92676) is a very potent and specific agonist for histamine H_2 receptors. *Nature (London)* **1978**, *276*, 403–405.

(22) Honrubia, M. A.; Vilaro, M. T.; Palacios, J. M.; Mengod, G. Distribution of the histamine H(2) receptor in monkey brain and its mRNA localization in monkey and human brain. *Synapse* **2000**, *38*, 343–354.

(23) Martinez-Mir, M. I.; Pollard, H.; Moreau, J.; Arrang, J.-M.; Ruat, M.; Traiffort, E.; Schwartz, J.-C.; Palacios, J. M. Three histamine receptors (H_1, H_2 and H_3) visualized in the brain of human and nonhuman primates. *Brain Res.* **1990**, *526*, 322–327.

(24) Martinez-Mir, M. I.; Pollard, H.; Moreau, J.; Traiffort, E.; Ruat, M.; Schwartz, J.-C.; Palacios, J. M. Loss of striatal histamine H_2 receptors in Huntington's chorea but not in Parkinson's disease: comparison with animal models. *Synapse* **1993**, *15*, 209–220.
(25) Traiffort, E.; Pollard, H.; Moreau, J.; Ruat, M.; Schwartz, J.-C.; Martinez-Mir, M. I.; Palacios, J. M. Pharmacological characterization and autoradiographic localization of histamine H_2 receptors in human brain identified with [^{125}I]iodoaminopotentidine. *J. Neurochem.* **1992**, *59*, 290–299.
(26) Brennauer, A. Acylguanidines as bioisosteric groups in argininamide-type neuropeptide Y, Y_1, and Y_2 receptor antagonists: synthesis, stability, and pharmacological activityPh.D. Thesis, University of Regensburg, Regensburg, Germany, 2006.
(27) Brennauer, A.; Dove, S.; Buschauer, A. Structure−activity relationships of nonpeptide neuropeptide Y receptor antagonists In *Handbook of Experimental Pharmacology*; Michel, M. C. , Eds.; Springer: Berlin, Heidelberg, New York, 2004; Vol. 162, pp 505−546.
(28) Schneider, E.; Keller, M.; Brennauer, A.; Hoefelschweiger, B. K.; Gross, D.; Wolfbeis, O. S.; Bernhardt, G.; Buschauer, A. Synthesis and characterization of the first fluorescent nonpeptide NPY Y1 receptor antagonist. *ChemBioChem* **2007**, *8*, 1981–1988.
(29) Feichtinger, K.; Sings, H. L.; Baker, T. J.; Matthews, K.; Goodman, M. Triurethane-Protected Guanidines and Triflyldiurethane-Protected Guanidines: New Reagents for Guanidinylation Reactions. *J. Org. Chem.* **1998**, *63*, 8432–8439.
(30) Stark, H.; Purand, K.; Hüls, A.; Ligneau, X.; Garbarg, M.; Schwartz, J.-C.; Schunack, W. [^{125}I]Iodoproxyfan and Related Compounds: A Reversible Radioligand and Novel Classes of Antagonists with High Affinity and Selectivity for the Histamine H_3 Receptor. *J. Med. Chem.* **1996**, *39*, 1220–1226.
(31) Mitsunobu, O.; Yamada, M.; Mukaiyama, T. Preparation of esters of phosphoric acid by the reaction of trivalent phosphorus compounds with diethyl azodicarboxylate in the presence of alcohols. *Bull. Chem. Soc. Jpn.* **1967**, *40*, 935–939.
(32) Götte, C. Synthese, Enantiomerentrennung und Struktur-Wirkungs-beziehungen neuer Histamin H_2 Rezeptoragonisten des Arpromidin TypsPh.D.Thesis, University of Regensburg, Regensburg, Germany, 2001.
(33) Preuss, H.; Ghorai, P.; Kraus, A.; Dove, S.; Buschauer, A.; Seifert, R. Point mutations in the second extracellular loop of the histamine H_2 receptor do not affect the species-selective activity of guanidine-type agonists. *Naunyn-Schmiedeberg's Arch. Pharmacol.* **2007**, *376*, 253–264.
(34) Preuss, H.; Ghorai, P.; Kraus, A.; Dove, S.; Buschauer, A.; Seifert, R. Mutations of Cys-17 and Ala-271 in the human histamine H2 receptor determine the species selectivity of guanidine-type agonists and increase constitutive activity. *J. Pharmacol. Exp. Ther.* **2007**, *321*, 975–982.
(35) Preuss, H.; Ghorai, P.; Kraus, A.; Dove, S.; Buschauer, A.; Seifert, R. Constitutive activity and ligand selectivity of human, guinea pig, rat, and canine histamine H_2 receptors. *J. Pharmacol. Exp. Ther.* **2007**, *321*, 983–995.
(36) Xie, S. X.; Petrache, G.; Schneider, E.; Ye, Q. Z.; Bernhardt, G.; Seifert, R.; Buschauer, A. Synthesis and pharmacological characterization of novel fluorescent histamine H_2-receptor ligands derived from aminopotentidine. *Bioorg. Med. Chem. Lett.* **2006**, *16*, 3886–3890.
(37) Xie, S.-X.; Ghorai, P.; Ye, Q.-Z.; Buschauer, A.; Seifert, R. Probing Ligand-Specific Histamine H_1- and H_2-Receptor Conformations with N^G-Acylated Imidazolylpropylguanidines. *J. Pharmacol. Exp. Ther.* **2006**, *317*, 139–146.
(38) Xie, S.-X.; Kraus, A.; Ghorai, P.; Ye, Q.-Z.; Elz, S.; Buschauer, A.; Seifert, R. N^1-(3-Cyclohexylbutanoyl)-N^2-[3-(1*H*-imidazol-4-yl)propyl]guanidine (UR-AK57), a Potent Partial Agonist for the Human Histamine H_1- and H_2-Receptors. *J. Pharmacol. Exp. Ther.* **2006**, *317*, 1262–1268.
(39) Gantz, I.; DelValle, J.; Wang, L. D.; Tashiro, T.; Munzert, G.; Guo, Y. J.; Konda, Y.; Yamada, T. Molecular basis for the interaction of histamine with the histamine H2 receptor. *J. Biol. Chem.* **1992**, *267*, 20840–20843.
(40) Ballesteros, J. A.; Weinstein, H. Integrated methods for the construction of three-dimensional models and computational probing of structure-function relations in G protein-coupled receptors. *Methods Neurosci.* **1995**, *25*, 366–428.
(41) Giraldo, J. A pH-dependent model of the activation mechanism of the histamine H2 receptor. *Biochem. Pharmacol.* **1999**, *58*, 343–353.
(42) Burde, R.; Seifert, R.; Buschauer, A.; Schultz, G. Histamine inhibits activation of human neutrophils and HL-60 leukemic cells via H_2-receptors. *Naunyn-Schmiedeberg's Arch. Pharmacol.* **1989**, *340*, 671–678.
(43) Shi, L.; Liapakis, G.; Xu, R.; Guarnieri, F.; Ballesteros, J. A.; Javitch, J. A. Beta2 adrenergic receptor activation. Modulation of the proline kink in transmembrane 6 by a rotamer toggle switch. *J. Biol. Chem.* **2002**, *277*, 40989–40996.
(44) Arrang, J. M.; Garbarg, M.; Schwartz, J. C. Auto-inhibition of brain histamine release mediated by a novel class (H3) of histamine receptor. *Nature (London)* **1983**, *302*, 832–837.
(45) Arrang, J. M.; Garbarg, M.; Schwartz, J. C. Autoinhibition of histamine synthesis mediated by presynaptic H3-receptors. *Neuroscience* **1987**, *23*, 149–157.
(46) Liu, C.; Ma, X.; Jiang, X.; Wilson, S. J.; Hofstra, C. L.; Blevitt, J.; Pyati, J.; Li, X.; Chai, W.; Carruthers, N.; Lovenberg, T. W. Cloning and pharmacological characterization of a fourth histamine receptor (H(4)) expressed in bone marrow. *Mol. Pharmacol.* **2001**, *59*, 420–426.
(47) Lim, H. D.; van Rijn, R. M.; Ling, P.; Bakker, R. A.; Thurmond, R. L.; Leurs, R. Evaluation of Histamine H_1-, H_2-, and H_3-Receptor Ligands at the Human Histamine H4 Receptor: Identification of 4-Methylhistamine as the First Potent and Selective H_4 Receptor Agonist. *J. Pharmacol. Exp. Ther.* **2005**, *314*, 1310–1321.
(48) Dove, S.; Michel, M. C.; Knieps, S.; Buschauer, A. Pharmacology and quantitative structure−activity relationships of imidazolylpropylguanidines with mepyramine-like substructures as non-peptide neuropeptide Y Y1 receptor antagonists. *Can. J. Physiol. Pharmacol.* **2000**, *78*, 108–115.
(49) Ziemek, R.; Schneider, E.; Kraus, A.; Cabrele, C.; Beck-Sickinger, A. G.; Bernhardt, G.; Buschauer, A. Determination of affinity and activity of ligands at the human neuropeptide Y Y4 receptor by flow cytometry and aequorin luminescence. *J. Recept. Signal Transduct. Res.* **2007**, *27*, 217–233.
(50) Schmuck, C.; Lex, J. Acetate Binding within a Supramolecular Network Formed by a Guanidinocarbonyl Pyrrole Cation in the Solid State. *Org. Lett.* **1999**, *1*, 1779–1781.
(51) Furchgott, R. F. The classification of adrenoceptors (adrenergic receptors). An evaluation from the standpoint of receptor theory In *Catecholamines*, Blaschko, H.; Muscholl, E. , Eds.;Springer: Berlin, Heidelberg, New York,1972; Vol. 33, pp 283−335.
(52) Arunlakshana, O.; Schild, H. O. Some quantitative uses of drug antagonists. *Br. J. Pharmacol. Chemother.* **1959**, *14*, 48–58.
(53) Van Rossum, J. M. Cumulative dose-response curves. II. Technique for the making of dose−response curves in isolated organs and the evaluation of drug parameters. *Arch. Int. Pharmacodyn. Ther.* **1963**, *143*, 299–330.
(54) Cheng, Y.; Prusoff, W. H. Relationship between the inhibition constant (K1) and the concentration of inhibitor which causes 50% inhibition (I50) of an enzymatic reaction. *Biochem. Pharmacol.* **1973**, *22*, 3099–3108.
(55) Rasmussen, S. G.; Choi, H. J.; Rosenbaum, D. M.; Kobilka, T. S.; Thian, F. S.; Edwards, P. C.; Burghammer, M.; Ratnala, V. R.; Sanishvili, R.; Fischetti, R. F.; Schertler, G. F.; Weis, W. I.; Kobilka, B. K. Crystal structure of the human beta2 adrenergic G-protein-coupled receptor. *Nature (London)* **2007**, *450*, 383–387.
(56) Wang, J.; Wolf, R. M.; Caldwell, J. W.; Kollman, P. A.; Case, D. A. Development and testing of a general amber force field. *J. Comput. Chem.* **2004**, *25*, 1157–1174.
(57) Lovell, S. C.; Word, J. M.; Richardson, J. S.; Richardson, D. C. The penultimate rotamer library. *Proteins* **2000**, *40*, 389–408.
(58) Halgren, T. A. Maximally diagonal force constants in dependent angle-bending coordinates. II. Implications for the design of empirical force fields. *J. Am. Chem. Soc.* **1990**, *112*, 4710–4723.
(59) Houston, C.; Wenzel-Seifert, K.; Bürckstümmer, T.; Seifert, R. The human histamine H_2-receptor couples more efficiently to Sf9 insect cell G_s-proteins than to insect cell G_q-proteins: limitations of Sf9 cells for the analysis of receptor/G_q-protein coupling. *J. Neurochem.* **2002**, *80*, 678–696.

JM800841W